Atmos. Chem. Phys. Discuss., 12, 17245–17293, 2012
www.atmos-chem-phys-discuss.net/12/17245/2012/
doi:10.5194/acpd-12-17245-2012

Atmospheric Chemistry and Physics Discussions

Evaluation of discrepancy between measured and modeled oxidized mercury species

G. Kos[1], A. Ryzhkov[2], A. Dastoor[3], J. Narayan[4], A. Steffen[4], P. A. Ariya[5], and L. Zhang[4]

[1]McGill University, Atmospheric and Oceanic Sciences, 801 Sherbrooke Street West, Montreal, QC, H3A 2K6, Canada
[2]Independent Researcher, 4998 Maisonneuve West, Westmount, QC, H3Z 1N2, Canada
[3]Air Quality Research Division, Environment Canada, 2121 Transcanada Highway, Dorval, QC, H9P 1J3, Canada
[4]Air Quality Research Division, Environment Canada, 4905 Dufferin Street, Toronto ON M3H 5T4, Canada
[5]McGill University, Atmospheric and Oceanic Sciences and Chemistry, 805 Sherbrooke Street West, Montreal, QC, H3A 2K6, Canada

Received: 29 May 2012 – Accepted: 31 May 2012 – Published: 12 July 2012

Correspondence to: A. Dastoor (ashu.dastoor@ec.gc.ca)

Published by Copernicus Publications on behalf of the European Geosciences Union.

Abstract

Zhang et al. (2012a), in a recent report, compared model estimates and new observations of oxidised and particulate mercury species (Hg^{2+} and Hg_p) in the Great Lakes region and found that the sum of Hg^{2+} and Hg_p varied between a factor of 2 to 10 between measurements and model. They suggested too high emission inputs and too fast oxidative conversion of Hg^0 to Hg^{2+} and Hg_p, as possible causes. This study quantitatively explores in detail the uncertainties in measurements, in addition to the above concerns and speciation of mercury near emission sources in the model to better understand these discrepancies in the context of oxidized mercury, i.e. gaseous (Hg^{2+}) and particulate (Hg_p) mercury. These include sampling efficiency, composition of sample, interfering species and calibration errors for measurements and in-plume reduction processes. Sensitivity simulations using Global/Regional Atmospheric Heavy Metals Model (GRAHM) were performed to analyze the role of in-plume reduction on ambient concentrations and deposition of mercury in North America. The discrepancy between simulated and observed concentrations of Hg^{2+} and Hg_p was found to be reduced when a ratio for Hg^0:Hg^{2+}:Hg_p in the emissions was changed from 50:40:10 (as specified in the original inventories) to 90:8:2 to account for in-plume reduction of Hg^0 processes. A significant reduction of the root mean square error (e.g., 19.22 to 11.3 $pg\,m^{-3}$ for New Jersey site NJ54) and bias (67.8 to 19.3 $pg\,m^{-3}$ for NJ54) for sampling sites in the Eastern United States and Canada, especially for sites near emission sources was found. Significant improvements in the spatial distribution of wet deposition of mercury in North America was noticed. Particularly, over-prediction of wet deposition near anthropogenic sources of mercury was reduced by 43 %. On a regional scale, estimated wet deposition improved by a factor of 2 for areas with more than 12 $\mu g\,m^{-2}$ yearly average wet deposition. Model sensitivity simulations show that the measured concentration of oxidized mercury is too low to be consistent with measured wet deposition fluxes in North America. This improvement by a factor of 2 and measurement uncer-

ACPD
12, 17245–17293, 2012

tainties within a factor of 3 to 8 provides a reasonable rationale for the discrepancy of a factor of 2–10 determined by Zhang et al. (2012a).

1 Introduction

Knowledge of the relationship between emission and deposition of atmospheric mercury is critical for the development of policies to reduce the levels of mercury in the environment (Wang et al., 2010b). While most mercury is present in the atmosphere in elemental form (Hg^0), other oxidized mercury species (mostly as Hg^{2+}) contribute significantly to overall processes due to their reactivity with other atmospheric species and constituents (Schroeder and Munthe, 1998). Both, elemental and oxidized mercury species in gaseous and particulate forms are emitted from anthropogenic sources into the atmosphere, while only gaseous elemental mercury (Hg^0) originates from terrestrial and oceanic (biogenic) sources (Lindberg and Stratton, 1998). Gaseous oxidized mercury (Hg^{2+}) is further produced from slow oxidation of elemental mercury in gas and aqueous phases (Liu et al., 2010). Low solubility and a comparatively long atmospheric lifetime of six months to one year results in global transport and slow deposition to the Earth's surface of Hg^0 (Schroeder and Munthe, 1998). Hg^{2+} and particle bound mercury (Hg_p) species, on the other hand, are removed by precipitation and surface uptake (dry deposition) at a much faster rate, i.e., within one to two weeks, making these species regional pollutants. Due to their solubility and reactivity, oxidised and particulate species are subject of a considerable body of research despite significantly lower concentrations ($ng\,m^{-3}$ for Hg^0 vs. $pg\,m^{-3}$ levels for Hg^{2+}/Hg_p; see e.g., Engle et al., 2010; Huang et al., 2010; Yatavelli et al., 2006; Poissant et al., 2005; Liu et al., 2011).

Many of the factors determining concentration changes of mercury species in the atmosphere remain poorly explored or unknown. On an emission level, the ratios of the emissions of Hg^0, Hg^{2+} and Hg_p species at the anthropogenic sources and oxidation-reduction processes in the emission plume and atmosphere at major point sources

ACPD
12, 17245–17293, 2012

(e.g., coal-fired power plants, CFPP) determine the speciation and reactions in the atmosphere (Seigneur et al., 2004). While atmospheric mercury reactions have been studied extensively, the impact of in-plume reactions on speciation is less known. While some previous studies suggest extensive reduction of Hg^{2+} in the plume by SO_2, currently neither laboratory nor field data exist to confirm the suggested reaction mechanism (Lohmann et al., 2006). As a consequence observations for oxidised and particulate mercury are required to determine the actual ratio of mercury species that will subsequently undergo tropospheric reactions.

For Hg_p, aerosol size distribution and composition are the major driver for processes involving particles, clusters and heterogeneous chemistry (Ariya, personal communication, 2011). Besides established aerosol research, the chemistry and properties of atmospheric ultrafine particles (UFP, <100 nm, also called nanoaerosols) have received growing attention in recent years (Justino et al., 2011). While it represents a small mass fraction of overall aerosol, its surface area and number density are considerable and, therefore, UFP are involved in heterogeneous chemical reactions and the formation of cloud condensation nuclei. While aggregates of UFP into clusters are greater in size, their properties are still distinct from aerosol particles of similar size, featuring a larger surface area for chemical reactions (Maynard and Aitken, 2007). Primary source of UFP are combustion, as hot exhaust gases mix with cooler air, and photochemically driven gas-to-particle formation processes. Detailed studies specific for mercury are not yet available to the author's knowledge.

Since the mercury deposition-characteristics highly depend on speciation, accurate determination of mercury fractions is key to the precise estimation of deposition near and away from the sources. An extensive network of mercury monitoring stations has been established in North America in recent years. The Mercury Deposition Network (MDN) monitors total mercury Hg_t concentrations from wet deposition over a large part of the continental US supplemented by Canadian stations (Prestbo and Gay, 2009). Measurement results agree reasonably well with model output data, typically within a factor of 2, because of a good correlation with precipitation data and the fact that no

ACPD
12, 17245–17293, 2012

mercury fraction analysis is performed (Ryaboshapko et al., 2007b). The MDN network has recently been supplemented by Atmospheric Mercury Network (AMNet) with the goal to provide fraction measurements to assess the impact of oxidised and particulate mercury species (Fitzgerald, 1995). Operational parameters and data management of AMNet are evolving with the goal of harmonizing protocols for better comparability (Steffen et al., 2012). AMNet has been providing oxidised and particulate mercury data in a structured fashion since 2009. Data analysis and model comparisons in this and previous studies rely mainly on AMNet datasets or pre-2009 datasets recorded at the same sites before the network was formally established.

The Tekran system is the most commonly employed analysis system for the determination of Hg^0, Hg^{2+} and Hg_p for AMNet and Canadian measurement sites. It combines automatic unsupervised long-term measurements with high sensitivity and field-based analysis (Atmospheric Mercury Network Site Operations Manual Version 1.0, 2011). Selective sample collection regimes are used to collect Hg^0, Hg^{2+} and Hg_p from the atmosphere. Since the system is the work horse for atmospheric mercury detection, its analytical performance has been well studied and a number of methodological uncertainties and limitations were identified (e.g. Swartzendruber et al., 2009; Slemr et al., 2009; Lyman et al., 2010). These include calibration non-linearity at low concentrations, and losses due to interference of oxidants and incomplete capture of Hg^{2+}. We aim to present a cumulative estimate for these uncertainties to better understand the variability of measurements.

Table 1 illustrates recent measurements of Hg^{2+} and Hg_p from different locations in the Northern Hemisphere. Hg^{2+} and Hg_p concentrations are often close to the instrument method detection limit (MDL; see Table 3). Both species concentrations are found at similar orders of magnitude and make up approximately 5 % of total atmospheric mercury. Studies aim to assess the regional impact associated with their short lifetimes (Weiss-Penzias et al., 2003b). Observation data show considerable variation with little correlation regarding geographic location stressing the importance of local sources (e.g. 8 $pg\,m^{-3}$ of Hg^{2+} at remote Ny Ålesund on Svålbard vs. 4 $pg\,m^{-3}$ in urban

ACPD
12, 17245–17293, 2012

Rochester, NY). The average Hg^{2+}/Hg_p ratio from these data is 0.85, illustrating the importance of particulate mercury species in atmospheric processes and the need for models to conform.

Environment Canada's Global/Regional Atmospheric Heavy Metals Model (GRAHM) simulates the emissions, transport, transformation and deposition of mercury species in the atmosphere (Dastoor and Larocque, 2004). Model estimates of ambient elemental and total gaseous mercury concentrations and wet deposition fluxes have been extensively evaluated in the past against observed data from North America and elsewhere on the globe (Sanei et al., 2010).

Until now, it was not possible to perform a comprehensive evaluation of model results, especially of Hg^{2+} and Hg_p species, mostly because of a lack of a sufficient body of measurement data. Recently, AMNet results were used in a comparative study of model estimates (Zhang et al., 2012a). In brief, output from three different mercury transport models including GRAHM were compared to AMNet measurement results from 14 sites in the Great Lakes region. Model results of Hg^{2+} and Hg_p at the 15 AMNet sites were overestimated by a factor of 2–10 for the sum of Hg^{2+} and Hg_p. Zhang et al. (2012b) provide several hypotheses for this discrepancy: (1) too high emission inputs; (2) too fast oxidative conversion of Hg^0 to Hg^{2+} and Hg_p; and (3) too low dry deposition velocities. While deposition velocities are discussed in some detail and not identified as the main source for the observed discrepancy, the authors suggest further investigation that led to the overestimation of the dry deposition results.

Currently, the modeling estimates of dry deposition velocities of mercury species are not constrained with observations; therefore it is difficult to use the limited measurements of dry deposition fluxes of mercury to evaluate the ambient concentrations of oxidized mercury. Moreover, measured dry deposition estimates are considered highly uncertain. Comparatively, ambient concentrations of Hg^0 and wet deposition fluxes of mercury have been extensively measured and are considered more reliable for constraining the models. Therefore, we make use of the measured wet deposition fluxes to constrain and evaluate the uncertainties in model estimated ambient concentrations of

ACPD
12, 17245–17293, 2012

oxidized mercury species in addition to the recent measurements of the oxidized mercury concentrations. Zhang et al. (2012a) employed the GEOS-Chem model for a validation of model results with AMNet data using a nested grid approach and obtained similar results. The presented study specifically addresses measurement uncertainties in conjunction with emission inventory and oxidation chemistry adjustments in order to provide a comprehensive synopsis of uncertainties on the measurement and model sides.

Figure 1 illustrates the differences between estimated and observed concentrations of Hg^{2+} and Hg_p simulated by a model version where only atmospheric dispersion and deposition of mercury were allowed without the production of oxidized mercury via atmospheric oxidation (NoChem; see Table 2 for details). Even without the chemistry, an over-prediction of up to 20 times for Hg^{2+} (for site NJ30 in 2009; see Table 4 for a detailed site description) and up to 7.6 times for Hg_p (site MD08 in 2009) is found. The presented study strives to explain reported discrepancies between observed Hg^{2+} and Hg_p concentrations by means of a detailed analysis of uncertainties for measurements and chemical reactions following emissions. The implications for model results are discussed and subsequently estimates of mercury budgets for North America from a revised version of GRAHM are presented.

2 Materials and methods

2.1 Model description

GRAHM is an Eulerian model built on top of Environment Canada's Global Environmental Multiscale-Global Deterministic Prediction System (Côté et al., 1998a, b). Meteorological and mercury processes are fully integrated in the GRAHM online chemical transport model. Mercury species described are Hg^0, Hg^{2+} and Hg_p. At each time step, mercury emissions are added to the atmospheric model concentrations, the meteorological processes are simulated, and the atmospheric mercury species are transported,

ACPD
12, 17245–17293, 2012

transformed chemically and deposited. GRAHM has been seen to perform well in past studies (Ryaboshapko et al., 2007a, b; Dastoor et al., 2008; Durnford et al., 2010). In the most model runs, gaseous oxidation of mercury by ozone occurs throughout the atmosphere with a temperature-dependent rate constant following Hall (1995).

In Ex-oxOH run (see Table 2) the ozone oxidation scheme was replaced with OH reaction using rate constants from Bullock and Brehme (2002) and Sommar et al. (2001) following the rationale of Lohman et al. (2006). The gaseous oxidation of mercury by halogens, including atomic and molecular chlorine and bromine as well as bromine oxide occurs in the marine boundary layer only. Rate constants are from Ariya et al. (2002), Raofie and Ariya (2003) and Donohoue et al. (2006). Mercury is reduced in the aqueous phase photochemically and by the sulfite anion and the hydroperoxyl radical using rate constants from Xiao et al. (1995), Pehkonen and Lin (1998) and Van Loon et al. (2000, 2001). Dry deposition is based on the resistance approach (Zhang et al., 2001, 2003). In the wet deposition scheme, Hg^0 and Hg^{2+} are partitioned between cloud droplets and air using a temperature-dependent Henry's law constant. We use the global anthropogenic mercury emission fields produced by AMAP for 2005 (Pacyna et al., 2010).

Emission ratios, especially the variability of the Hg^0:Hg^{2+}:Hg_p ratio at the stack and subsequent reactions in the plume, seem to be among the most important parameters and processes that need modification to better represent atmospheric oxidized and particulate mercury concentration. In the absence of better knowledge of emission speciation and in-plume chemistry, several model runs were conducted by changing the emission ratios of emitted Hg species at the sources. Resulting ratios are listed in Table 2. Non-anthropogenic terrestrial and oceanic emissions of Hg^0 are based on the global mercury budget of Mason (2009). Horizontal resolution of the model runs was 1° unless otherwise indicated.

ACPD
12, 17245–17293, 2012

2.2 Atomic fluorescence spectrometer setup and sampling

While several methods for the measurement of mercury species in the atmosphere have been developed (Munthe et al., 2001), the most popular methodology for field-deployed systems and continuous monitoring is the detection of mercury species using cold vapor atomic fluorescence spectrometry (CVAFS) (Bloom and Fitzgerald, 1988). The widely employed Tekran 2537A analyzer system quantifies mercury species as Hg^0 after amalgamation and concentration on a gold surface followed by thermal desorption into the CVAFS analysis system.

Mercury fractionation, commonly called "speciation", although the "species" definition for Tekran measurements is strictly operational, is achieved using two different inline sampling protocols, for Hg^{2+} and Hg_p species. KCl-coated annular denuders made of quartz are most commonly used for Hg^{2+} at air sample flow rates of 10 l min^{-1} leading to the collection of species on the modified denuder surface, followed by thermal desorption and detection. Hg_p is deposited on a quartz filter surface followed by pyrolysis and detection (Lindberg et al., 2002). A combination setup was commercialized by Tekran as systems 1130 (Hg^{2+}) and 1135 (Hg_p) speciation units, which are now used for Hg concentration monitoring. Samples are sequentially desorbed from the collection device and analysed as Hg^0 after reduction using CVAFS. Table 3 lists sampling times for Hg^{2+} and Hg_p which are comparatively long (hours vs. typically 5 min for Hg^0) due to the low concentrations observed (Landis et al., 2002). The table also illustrates the large variability of sampling times and resulting differences in the method detection limit (MDL), which is difficult to estimate due to lack of standards for Hg^{2+} and Hg_p. The MDL is certainly dependent on sampling time and this the quantity of material collected for analysis and varies between 1 and 4 pg m^{-3}. The MDL is not always specified separately for Hg^{2+} and Hg_p and the mode of calculation is rarely reported. A better documented rationale for Hg^{2+} and Hg_p MDLs is desirable since observed concentrations are often, if not mostly, below or around the MDL for both species and actively being addressed (Steffen et al., 2012).

ACPD
12, 17245–17293, 2012

Measurement data and the range for yearly means used for analysis in this study are listed in Table 4 and represent an expanded data set including but not limited to sites from Table 3 in order to allow for a comparison on a continental scale and maintain comparability with results from Zhang et al. (2012a). Data from 21 sites were analysed with 2 colocated instruments for a total of 41 yearly datasets from 2002 to 2010. A minimum of 7 seven months of observations per year was required for a data set to qualify for consideration. Colocated data were treated as coming from a single location, i.e. for MS12 and NY43, respectively also shown in Fig. 2.

Estimations from the model base run and modified runs were compared with observations by calculating the unbiased root mean square error (URMSE) and Bias for yearly means and the correlation of weekly averaged data for time series analyses. Observation data was obtained from principal investigators and consisted of blank corrected, but not MDL censored concentrations from individual CVAFS runs. Missing data were marked as "not available" (NA) for calculations, zero data as a result of blank correction were kept as is. Negative data as a result of blank correction were replaced by zero. Kaplan-Meier (KM) methods were employed for all calculations to avoid the introduction of a bias by arbitrarily assigning zero or 0.5 MDL to data below the reporting limit (Helsel, 2005). KM daily, weekly and monthly means were compared to corresponding arithmetic means from model estimates (not shown). For sets with data points above the MDL (e.g. for Hg^0) no significant difference was observed, but for Hg^{2+} and Hg_p data up to 80 % was < MDL resulting in differences for mean and median values. Statistical calculations and analyses were carried out employing R 2.13.

3 Results and discussion

3.1 Uncertainty of measurements

Atmospheric mercury measurement data from 15 sites around the Great Lakes region and the Eastern United States were used by Zhang et al. (2012a) for comparison

ACPD
12, 17245–17293, 2012

with model estimates. These data and the additional data used in this study were collected as part of AMNet and Environment Canada sampling and measurement stations and were in reasonable agreement regarding instrumentation and operating parameters (see Table 3 for remarks, Hg^{2+} and Hg_p sampling times show some notable differences). Most importantly, all experiments were carried out using the same type of instrumentation, thus eliminating uncertainties arising from different measurement principles, including species measured. Nevertheless, the employed sample collection and analyte detection method leads to significant uncertainties associated with the data, which will be discussed with a focus on Hg^{2+} and Hg_p, where due to low observed concentrations near the MDL the impact is most significant (Sigler et al., 2009).

The immediate sampling environment including inlet position of CVAFS sampling devices has a pronounced influence on Hg^{2+} concentrations. Forested areas tend to scrub Hg^{2+} concentrations in its surroundings leading to underestimation, when applying these concentrations to estimate concentrations above the canopy. Hence, results might not be representative for regional and larger scale predictions and, therefore, less suited for comparison (Prestbo, personal communication, 2011). The change of Hg^{2+} concentrations with altitude has not yet been studied in detail and the effect of the immediate sampling environment on the Hg^{2+} concentration gradient from above to below the canopy is unknown. There are some indications that concentrations are higher with increasing altitude, but a statistical analysis has not been performed for lack of data. Concentration differences for Hg^{2+} measured with refluxing mist chambers were a factor of 4 apart (Lindberg and Stratton, 1998). Because of these local, sub-grid effects, it can be assumed that some observations do not correspond to surface layer concentrations estimated by models.

3.2 Hg^{2+} sampled as Hg^0

Hg^0 concentrations only are often measured with a Tekran 2537A unit without the speciation units (e.g. EC CAMNet) and higher concentrations were observed for Hg^0 compared to combination systems with denuder and quartz filter setups. At Alert, NU Hg^0

ACPD
12, 17245–17293, 2012

data is available from both systems and significant differences are observed. It is unclear, if co-sampled Hg^{2+} is the reason, since precautions (e.g. long sample lines) are taken to avoid cross-contamination (Steffen, personal communication, 2011). For Hg^0 differences were calculated to be 18 % with a yearly average of 1.53 ng m^{-3} for the standalone instrument vs. 1.26 ng m^{-3} for the combination system in 2005. As a consequence CAMNet data from standalone instruments are reported for Hg^0 concentrations at Alert and supplemented with Hg^{2+} and Hg_p data from the combination system. These data sets were also used for calculations in this study.

Reports indicate that Hg^{2+} tends to be measured together with Hg^0 for some inlet configurations and environmental conditions. Hg^{2+} species have the tendency to stick to surfaces as demonstrated for $HgCl_2$, and it is, therefore, thought to be analysed with Hg^0 species. As a result a mercury concentration will be closer to total gaseous mercury, the sum of Hg^0 and Hg^{2+}. While the combination systems eliminate this drawback by sampling Hg^{2+} and Hg_p right after the inlet, care has to be taken, when comparing data coming from different sources and systems to account for operational differences.

3.3 Hg^{2+} Sampling uncertainties

Since the true composition of Hg^{2+} is unknown a detailed assessment of quantitative sampling of Hg^{2+} is impossible (Selin et al., 2009). Major species that are assumed to be part of Hg^{2+} are $HgCl_2$, $HgBr_2$ and HgO (Munthe et al., 2001; Aspmo et al., 2005; Lyman et al., 2010) and Hg^{2+} is (operationally) defined as watersoluble oxidised mercury species (Landis et al., 2002) that can be reduced by stannous chloride in aqueous solutions without pretreatment (Munthe et al., 2001). Reactive gaseous mercury (RGM) is a commonly used alternative term for these species. Other candidate compounds suggested for the Hg^{2+} component pool are cross halogen species with chlorine, bromine and iodine atoms (Ariya, personal communication, 2011). Their contribution to the overall Hg^{2+} concentration is unknown and no literature data exists.

ACPD
12, 17245–17293, 2012

$HgCl_2$ is commonly employed as a model compound for Hg^{2+} to evaluate method performance, since it is a thermodynamically favoured product of fossil fuel and waste combustion facilities (Landis et al., 2002 citing Klockow et al., 1990). As a consequence the full composition of the Hg^{2+} fraction captured by the annular denuder setup is not known (Lindberg et al., 2007; Landis et al., 2002); it has been reported that species with diffusion coefficients $> 0.1\,cm^2\,s^{-1}$ are typically measured (Poissant et al., 2005). No further quantitative data is available, making a quantitative error analysis not feasible.

3.4 Hg_p Sampling and aerosol size distribution

For Hg_p sampling a quartz filter with an upper size cut off at 2.5 µm is employed (Landis et al., 2002). This raises issues with both, ultrafine (UFP) and large particle fractions of the total aerosol distribution. For particles > 2.5 µm, Keeler et al., 1995 showed bimodal distribution with a second maximum at 3.8 µm for some samples indicating that a significant portion of mercury species from larger aerosol fractions are potentially not collected and reported as Hg_p. The lower size cut off is less clearly defined. Mercury adhering to UFP shows gas-like behaviour despite its particulate character thus potentially misclassifying Hg_p as Hg^0 and Hg^{2+} (Ariya, personal communication, 2011). The distinct character of UFP and its clusters apart from classic aerosol has been recognized as has its potential for heterogeneous chemistry reactions due to the large surface area. Mercury has not been determined in UFP and the degree of underestimation by current sampling methodologies are not known.

Furthermore, for 1-h sampling durations elevated temperatures in the filter assembly (typically 50 °C to exclude moisture) have been shown to lead to identification of Hg_p as Hg^{2+} (Rutter and Schauer, 2007). Prolonged collection times of up to 12 h as they often occur to reach the filter loadings necessary for detection led to filter losses for Hg_p (Malcolm and Keeler, 2007). Collection times for the discussed studies were typically lower (1–3 h; see Table 3), thus minimising the risk for filter losses.

ACPD
12, 17245–17293, 2012

3.5 Ozone interference during sampling

Recently, the impact of the presence of ozone on Hg^{2+} sampling using the denuder technique was investigated (Lyman et al., 2010). Significant loss of oxidized mercury ($HgCl_2$, $HgBr_2$) as elemental mercury was observed in laboratory experiments (39–55 % loss) and at a field site (3–37 %). Precision of replicate denuder measurements was determined to be around 30 %. Additionally collection efficiency of denuders for $HgCl_2$ decreased by 12–30 % in the presence of ozone. Hence, any Hg^{2+} will subsequently be detected as Hg^0 employing the combination setup with the denuder sampling device placed upstream of the Hg^0 detection unit. Further investigation of ozone and other potential interfering oxidising species such as peroxides is recommended.

3.6 Instrumention-related uncertainties

While AMNet has made considerable progress towards harmonisation of instrument operation, earlier data was not necessarily acquired in a fully standardised fashion. Different operating parameters might compromise comparability of data. These issues are being addressed by an AMNet standard operating procedure (Steffen et al., 2012).

Among the issues to be addressed is the 2-point calibration at 0 and 15 ng sm^{-3} that the Tekran system uses, and for low concentrations problems with linearity of the calibration curve were previously reported (Swartzendruber et al., 2009). Since low concentrations (in the pg m^{-3} range) are typically observed for Hg^{2+} and Hg_p, a thorough assessment of linearity is especially important for these species. Hg^0 measurement uncertainty was reported to be 12–20 % (2 s), which has direct implications for Hg^{2+} and Hg_p, since these species are ultimately detected as Hg^0 (Aspmo et al., 2005; Temme et al., 2007; Brown et al., 2008).

A good assessment of the method detection limit (MDL) is imperative for the same reasons. Sampling for Hg^{2+} and Hg_p typically takes 1–3 h followed by 1 h of desorption and analysis (sum equals “cycle time”). Landis et al. (2002) found MDLs of 6.2 pg m^{-3}

ACPD
12, 17245–17293, 2012

and 3.1 pg m^{-3} for Hg^{2+} for sampling durations of 1-h and 2-h at 10 l min^{-1} sample flow rate.

For the reviewed literature in Table 2 reported MDLs were around 1 pg m^{-3} and considerably lower than Landis' study. In discussions with instrument operators values between 2 and 5 pg m^{-3} were reported (Tate et al., 2011; Steffen et al., 2011; Eckley et al., 2011; all personal communication). Due to a lack of suitable standards MDL calculations are not straightforward and 3 times the standard deviation of the blank is most often used, but deemed problematic due to large fluctuations of the blank. Operator experience was cited as a better, but not objective means for what data could be trusted (Eckley, personal communication, 2011). Separate MDLs for Hg_p are rarely specified. Depending on the MDL used for statistical calculations, a significant fraction (up to 40–80 %) of Hg^{2+} and Hg_p data falls below the MDL with implications for interpretation and statistical procedures used (Engle et al., 2010). The uncertainty in establishing a suitable MDL together with data near the MDL highlights the challenges that a reliable determination of Hg^{2+} and Hg_p face.

The precision of the denuder method was determined by the collection of colocated samples ($n = 63$) to be 15.0 ± 9.3 % (Landis et al., 2002). Precision for automated 1130/1135 methods is, according to Poissant et al. (2005) unknown and usually not listed.

3.7 Statistical treatment of observational data

With a large number of observations and observed concentrations at the MDL a suitable treatment of data has to be employed to account for non-detect data. In the current literature environmental data are either used as-is or undergo some form of treatment, e.g. substitution with a fraction of the MDL, typically one-half, for values <MDL (Helsel, 2005). A considerable loss of information is the consequence, together with the potential introduction of a biased estimate fabricated data. In conjunction with the MDL used as a criterion for censoring data significant differences and reliability of results

ACPD
12, 17245–17293, 2012

can occur. For example raw data from Poissant et al. (2005) at St-Anicet, QC has a reported MDL of 3.75 pg m^{-3}. Due to its more rural location a much smaller number of data points is >MDL (22.2 %). Median and mean values are different for Kaplan-Meier treated data censoring at the MDL compared to classical statistics calculating the arithmetic mean and median: the median changes from 1.27 with classical treatment to 0.82 pg m^{-3} for Kaplan-Meier treated data. The change of the mean is smaller from 3.32 to 3.20 pg m^{-3}. Concluding, a standardised procedure of data treatment has to be agreed upon that treats non-detects in a suitable fashion and takes into account instrument-specific MDLs. Methods such as robust statistics, Kaplan-Meier estimates and maximum likelihood estimation (MLE) are much more suitable for the treatment of censored environmental data (Helsel, 1990), especially for Hg^{2+} and Hg_p concentrations, which are often found to be below the detection limit (Engle et al., 2010). Table 5 describes uncertainties for CVAFS measurements together with other sources of uncertainty related to emissions and atmospheric chemistry processes. Regarding measurements, individual parameter assessments, e.g. for accuracy and precision of the denuder sampler, are typically not available, because of a lack of standards (Aspmo et al., 2005), but some estimates exist regarding the cumulative uncertainty of Hg^{2+} and Hg_p measurements.

3.8 Emission uncertainties

Current emission inventories prescribe a fixed Hg^0:Hg^{2+}:Hg_p emission ratio for any CFPP, currently 50 %:40 %:10 % (EPA year/UNEP year). Stack data, however, indicates a large variability of the mercury species ratios between CFPPs, depending on multiple parameters such as air pollution control devices (APCD) used and the mercury content of coal burned at a given time (Hsi et al., 2010). Such variations are not accounted for in inventories.

Measurements of mercury species at observation sites near CFPPs revealed that there was indeed a large variability in e.g. Hg^{2+} emissions ranging from 5 to 35 % during different plume events at a sampling site with three CFPPs within a <60 mile radius

ACPD
12, 17245–17293, 2012

and 4 to 29 % for a sampling site with a single CFPP within 15 miles (Edgerton et al., 2006). Quite variable data on mercury species' contributions to flue gas composition were also recently published for South Korea showing differences between bituminous coal (Hg^{2+}: 0.73 $\mu g\,m^{-3}$ after treatment) and anthracite (1.41 $\mu g\,m^{-3}$) for CFPPs and treatment of flue gas using wet or dry APCD. Dry APCDs were reported to lead to higher Hg^{2+} concentrations, whereas wet treatment yielded less oxidised effluent gas (Kim et al., 2010). Even more variability was described for other incinerating facilities with Hg^{2+} concentrations in the flue gas after treatment being as 190 $\mu g\,m^{-3}$ for industrial waste incinerators. Wang et al., 2010 also reported significant variability of Hg^{2+} concentrations from different CFPP after flue gas treatment (0.13 to 24 $\mu g\,m^{-3}$). Analysis of coal composition is also provided including correlation of Hg^{2+} with halogen content of the coal confirming previous studies that reported increased conversion to Hg^{2+} at high halogen content (e.g. Niksa et al., 2009). A summary of Hg^{2+} concentrations ranging from 2–76 % in coal with 37 to 510 $\mu g\,kg^{-1}$ total Hg including work by the authors also provides information on coal used and APCDs in place (Shah et al., 2010). Additionally modeled emission estimations for Chinese provinces by Wu et al. (2010b) indicated a high uncertainty for Hg^{2+} of up to a factor of 3.

3.9 Uncertainties associated with chemistry knowledge gap

CFPPs are considered the major source of anthropogenic mercury emissions due to the natural occurrence of mercury in coal at trace levels (Wang et al., 2010a). Emitted mercury then undergoes reactions with a multitude of chemical species (Shah et al., 2010). After release from the stack, there are experimental and model indications that plume chemistry considerably changes the Hg^0:Hg^{2+}:Hg_p ratio. Observations from a CFPP at Nanticoke, ON show large stack concentrations of Hg^{2+} compared to emissions measured in the plume that are rapidly reduced to an approximate ratio of 90 %:5 %:5 % within a few minutes (Deeds, personal communication, 2011). Lohman et al. (2006) and Vijayaraghavan et al. (2008) have previously modeled the reduction

ACPD
12, 17245–17293, 2012

of Hg^{2+} to Hg^0 in the presence of SO_2. In some cases plant specific emission estimates were used for modeling, were still quite different from observations, suggesting additional mechanisms such as reductive plume chemistry and depositional losses (Edgerton et al., 2006).

There is also evidence for Hg^{2+} adsorption on particles (Rutter and Schauer, 2007) and an adsorption mechanism was introduced into initial model calculations resulting in a ground-level Hg^{2+} reduction by 23 % (Vijayaraghavan et al., 2008). Both mechanisms, if implemented in model calculations could reduce Hg^{2+} estimates significantly.

A recent modification of the GEOS-Chem global mercury transport model introduced atomic bromine chemistry as an alternative oxidant for Hg^0 and compared it to established OH/O_3 processes (Holmes et al., 2010). The authors suggest a reduction of the Hg^0 to Hg^{2+} oxidation rate by 60 % to bring results in line with observations on a global scale. This reduction is within estimated uncertainties for the oxidation of HgBr to HgBrX (X≡Br, OH) (Goodsite et al., 2004; Balabanov et al., 2005). Holmes et al. (2010) also suggests photochemical reduction in clouds as possible alternative. CFPP-tailored emission ratios, in-plume Hg^{2+} reduction by SO_2 and Hg^{2+} adsorption to particulates have recently been integrated into mercury transport models, but are not yet commonly employed (Zhang et al., 2012a). The significance of plume chemistry and atmospheric reduction processes (e.g. gas phase reactions, heterogeneous chemistry and aqueous chemistry) need to be further investigated as they could have a significant impact on Hg^{2+} and H_p concentrations that will in turn affect model estimations (Lohman et al., 2006).

3.10 Summary of uncertainties

The uncertainty knowledge gap originates from measurement and laboratory errors, lacking representation of plume and atmospheric chemistry processes in models and emission inventory uncertainties, all of which are listed in Table 5. A quantitative summary estimate is difficult to achieve since the modes of calculation vary by author and

ACPD
12, 17245–17293, 2012

are usually not made transparent. However, a number of uncertainties lead to lower measurement data, which could help closing the gap between potentially overestimated model data and underestimated observations. Among these are the following items for Hg^{2+} in Table 5: position of the sample inlet (item 2), incorrect baseline integration (item 6), ozone interference (items 7 and 8), and in-plume reduction and adsorption processes (items 16 and 17). Without the first item the sum of uncertainty factors that are exclusively lowering Hg^{2+} observations is 143 %. Including general measurement uncertainties (items 9, 10) and differences during colocation experiments (items 2, 3, 5) of 20 % each, underestimation could reach 200 %, still not considering sample inlet height, which could lead to an underestimation of up to an additional 400 %. Emission related uncertainties (items 11–14) could contribute another 50 % to the cumulative uncertainty. Despite this crude summary, the assumption that Hg^{2+} concentrations could be underestimated by a conservatively estimated factor of 2–3 holds, and could be up to a factor of 8 taking into account all variations at their maximum impact. Table 5 demonstrates clearly, that eliminating the discrepancies between model estimates and observations and reducing uncertainties requires additional efforts from both, modeling and measurement communities. The presented analysis provides starting points to address in the improvement of analytical and emission data: (1) choice of sampling locations and heights well represent atmospheric Hg^{2+} concentrations, also at sources, (2) assessment of interferents such as ozone (3) elimination of data analysis related to low Hg^{2+} and Hg_p concentrations and (4) improved treatment of CFPP emission estimates with regard to coal burned and flue gas treatment systems.

3.11 Model sensitivity analysis

Figures 3 and 4 present surface air mean, median and variance of yearly averaged Hg^0, Hg^{2+} and Hg_p concentrations and wet deposition fluxes between all sites estimated by base simulation, experiments and the measurements.

Average modeled median for Hg^0 is slightly higher in the Ex-oxOH run by 0.13 ng m^{-3}, whereas variation is somewhat smaller which is related to the representa-

ACPD
12, 17245–17293, 2012

tiveness of the resolution of the model. The Hg^0 concentrations are seen to be invariant between experiments; however absence of Hg^0 oxidation processes in the atmosphere lead to unrealistically high values of Hg^0. Observed averaged mean Hg_p concentration is slightly higher compared to the averaged mean Hg^{2+} concentration; however observed averaged median Hg_p concentration is lower compared to averaged mean Hg^{2+} concentration. Also, observed Hg^{2+} concentrations are more uniform within the domain (low variation) compared to the variability in Hg_p concentrations. The experiment with no production of Hg^{2+} through atmospheric chemistry (NoChem experiment) results in significantly higher spatial variation and yearly mean concentrations of Hg^{2+} ($30.02\,pg\,m^{-3}$) compared to observed ($7.172\,pg\,m^{-3}$). Hg_p mean and median concentrations are only slightly elevated compared to measured values; whereas the variance between sites is higher compared to measurements. When no emission of Hg^{2+} is considered (NoEmit experiment), the chemistry alone produces lower concentrations of Hg_p, however Hg^{2+} concentrations are still overestimated compared to observation. Chemically produced Hg^{2+} and Hg_p concentrations are found to be very uniform across the domain. The wet deposition fluxes are underestimated in both cases and lack variation compared to measurements. A point to note here is that while both Hg^{2+} and Hg_p mean concentrations are simulated to be higher in the NoChem experiment compared to the NoEmit experiment, the wet deposition is simulated to be markedly lower in the NoChem experiment compared to the NoEmit experiment. This is because the emissions increase Hg^{2+} close to the surface, where it can be readily dry deposited; however chemistry produces Hg^{2+} aloft that is scavenged into clouds and wet deposited. These experiments suggest that spatial distribution of ambient Hg^{2+} concentrations is more likely to be generated by slow oxidative processes whereas Hg_p species is produced both through emission and chemistry. Based on the no chemistry and no emission experiments, it can be inferred that the variability in base simulation is mostly due to the primary emissions of Hg^{2+} which is higher compared to measurements. Next experiment (Ex-ox1), where the emission ratios were modified to 90:8:2 (Hg^0:Hg^{2+}:Hg_p)

ACPD
12, 17245–17293, 2012

is seen to produce mean Hg^{2+} concentrations higher by a factor of two compared to the observed mean; however median Hg_p concentrations are slightly underpredicted. Although the bias in Hg^{2+} and Hg_p is much smaller, the wet deposition fluxes are significantly underpredicted ($-4.3\,\mu g\,m^{-2}$). It should be noted that the variance is reduced in all three variables, most notably in Hg^{2+} concentrations which is in line with observations. The oxidation rate was doubled in the next experiment (Ex-ox2) to see the impact on wet deposition fluxes. This experiment produced wet deposition fluxes comparable to the observed values; however Hg^{2+} concentrations are increased by 60 %, whereas Hg_p concentrations agree well with the observed values. In the next experiment (Ex-oxOH), OH was used as the main oxidant and ozone oxidation was not considered. The mean concentrations Hg^0, Hg^{2+} and Hg_p were found to be comparable to ozone oxidation experiment with twice the oxidation rate estimated by Hall (1995); however the spatial distribution of the species and wet deposition fluxes, particularly the North South gradient in wet deposition was improved when OH oxidation was used. In EX-ox1.5-CFPP experiment, the emission ratios for Coal Fired Power Plants (CFPP) alone were modified to 90:5:5 (Hg^0:Hg^{2+}:Hg_p); although the bias is reduced for both Hg^{2+} and Hg_p concentrations compared to the base run, very high concentrations of Hg^{2+} at several sites and overestimation of Hg_p concentrations were simulated. Another experiment (Ex-ox2-HiHgp) was conducted where the Hg^{2+}/Hg_p partitioning was modified from 0.75 to 0.25 (Table 2). This experiment resulted in over-prediction of Hg_p as well as wet deposition. Overall, OH as dominant oxidation scheme for Hg^0 with 90:8:2 emission ratios for Hg^0:Hg^{2+}:Hg_p produced best results. Changing emission ratios to 90:8:2 not only reduces the bias in Hg^{2+}, it also reduces the spread in the bias (Fig. 4b), whereas there is no significant change in the spread of the bias in Hg_p concentrations (Fig. 4c). This difference between Hg^{2+} and Hg_p is likely due to the fact that primary emissions of Hg^{2+} are much higher in the original emissions inventory (40 %) compared to the emissions of Hg_p (10 %) used in the base simulation. It is important to note that higher

ACPD
12, 17245–17293, 2012

atmospheric concentrations of Hg^{2+} are needed compared to measured estimates in order to simulate the observed levels of wet deposition fluxes.

The results shown in Figs. 3 and 4 are further analyzed in Fig. 5. The Hg^{2+} and Hg_p concentrations estimated by the experiment without chemistry (NoChem; x-axis) were plotted against the Hg^{2+} and Hg_p concentrations of base simulation (base; red) and OH oxidation and modified emission ratio experiment (Ex-oxOH; blue). Since distribution of Hg^{2+} in the NoChem experiment is determined by the dispersion of these species from the emission sources only, higher concentrations on the x-axis represent proximity to the emission sources. Figure 5 clearly illustrates linearly increasing bias in Hg^{2+} concentrations in the base simulation closer to the sources of emissions. Although the Hg^{2+} bias is significantly reduced with modified emission ratios (blue), it is still found to slightly increase near sources. Lowering the emission of Hg_p is also found to correct the larger bias in Hg_p closer to the sources; however the correction leads to negative bias at some of the sites. The negative bias at these sites including Alert, is perhaps due to improper partitioning between Hg^{2+} and Hg_p. Impact of lowering the primary emissions of Hg^{2+} is also pronounced in weekly averaged data for sites close to mercury sources, such as NJ54 and NJ 30. The bias is lowered from 67.8 to 19.8 $pg\,m^{-3}$ for Hg^{2+} and the unbiased root mean square error (URMSE), drops from 19.22 to 11.3 $pg\,m^{-3}$ for Hg^{2+} at the NJ54 site. Thus, not only yearly means, but also temporal variations from weekly averaged data are markedly improved.

Figure 6 illustrates the spatial pattern of Hg^{2+}, Hg_p and wet deposition for the base run and the best run with high 90 % Hg^0 emissions and OH oxidation. Hg^{2+} is noticeably high in the base run in the vicinity of sources compared to the observed values. The Ex-oxOH run is clearly seen to be markedly improved. The most notable improvement is seen in the wet deposition which has a N–S gradient in the observations. The base run produces very high wet deposition fluxes in the vicinity of sources; whereas this discrepancy is corrected in the best run. The N–S gradient is reproduced well in the Ex-OH experiment. This is also the case with simulation using ozone as the main oxidant. N–S gradient and high wet deposition fluxes in the South-Eastern United States

ACPD
12, 17245–17293, 2012

are a combination of chemically produced Hg^{2+} in the free troposphere, gradient in precipitation and scavenging of Hg^{2+} by high cumulus clouds (Selin and Jacob, 2008). These results suggest that Hg^{2+} is dominantly produced by chemistry and does not seem to be dependent on primary emissions, and perhaps aerosol distribution in the atmosphere that would control the partitioning between the Hg^{2+} and Hg_p concentrations. Since wet deposition is generated through the scavenging of oxidized mercury species and is known to have lower measurement uncertainties compared to the Hg^{2+} and Hg_p measurements currently, good agreement between observed and modeled spatial distribution and fluxes of wet deposition suggest that atmospheric concentrations of Hg^{2+} should be higher than current estimates from the observations.

3.12 Detailed wet deposition analysis

Wet deposition occurs by the scavenging of the oxidized mercury in and below cloud hydrometeors. Measured wet deposition fluxes are currently considered to be accurate within 20 % (Bullock, 2009). Figure 7 shows a high-resolution (0.15°) wet deposition map plot. Circles contain observational data. For Ex-oxOH estimations results are markedly improved compared to Fig. 6f for high concentration areas such as the Southern United States. Figure 8 presents the scatter plot of annual wet deposition flux for 2005 between observed (MDN) and three model runs (base, Ex-ox2 and Ex-oxOH). The intercept (i), slope (m) and correlation coefficient (r^2) improved from base run (i = 4.76, m = 0.33, r^2 = 0.26) to Ex-ox2 (i = 4.36, m = 0.50, r^2 = 0.53) to Ex-oxOH (i = 2.63, m = 0.61, r^2 = 0.66). Comparison of the monthly wet deposition fluxes for the three model runs (base, Ex-ox2 and Ex-oxOH) with MDN reveals that using the OH oxidation chemistry in conjunction with anthropogenic emissions as mostly Hg_0 species improves the seasonal cycle throughout the year particularly in the North East and South East North America (Fig. 9).

ACPD
12, 17245–17293, 2012

4 Conclusions

The presented study provides a detailed global analysis of uncertainties associated with mercury transport measurements and modeling for 21 sampling sites throughout North America and a total of 38 yearly datasets acquired between 2002 and 2010. A total uncertainty factor of up to a factor of 8 was determined from a combination of instrument-, measurement- and emission-inventory-related uncertainties. The highest uncertainty (factor 4; with very limited availability of data) was identified to be the position of the sample inlet and the immediate sampling environment, to cause scrubbing of reactive mercury species and non-representative values for comparison with model estimates for the bottom layer. Furthermore, there are contributions from variations of coal burned in power plants (factor 2–4) and significant underestimation of reactive mercury due to interference of ozone (up to 50 %). Published data from co-located measurements show differences of up to 40 %.

Concerning model-related overestimation of reactive mercury species (Hg^{2+} and Hg_p) a significant reduction of the bias was achieved after a comparison of yearly means and measurement data at the same sampling sites, thus extending the validation of model estimates to a continental scale. Improvements were especially significant for urban (near sources) sites in New Jersey, where bias values dropped from 67.8 to 19.8 (NJ54) and 87.7 to 25.4 (NJ30), while the good estimation of Hg^0 data was not affected. The improvements for yearly means was confirmed by time series analysis of weekly means showing the same trends. Significant changes made to model parameters were the adjustment of emission ratios to Hg^0:Hg^{2+}:Hg_p to 90:8:2 to account for plume chemistry processes that were observed at Nanticoke, ON and modeled in earlier studies. Furthermore, the previously used ozone oxidation scheme was replaced by hydroxyl radical oxidation. This lead to a considerable improvement of estimated wet deposition data, which was evaluated on a regional scale. Significant gains were made for previously underestimated high precipitation areas with estimated results improved by a factor of 2.

ACPD
12, 17245–17293, 2012

We conclude that the remaining discrepancy between modeled and observed Hg^{2+} (about 2 times higher) is within the limits of errors in observations of Hg^{2+} and Hg_p concentrations. Major questions regarding plume chemistry and atmospheric mercury reduction reactions in the gas-, aqueous phases and heterogeneous chemistry remain that could have a major impact once these mechanisms are better understood and implemented in transport models. It is also important to obtain more reliable Hg^{2+} and Hg_p concentration data and reduce significant uncertainties for these trace concentration measurements.

Acknowledgement. The authors kindly acknowledge C. Banic (Environment Canada), D. Deeds (McGill University), C. Eckley (Environment Canada), M. Engle (USGS), E. Prestbo (Tekran Inc.), and M. Tate (USGS) for insightful discussions on plume chemistry, aerosol chemistry and atmospheric reduction processes of mercury species. We extend thanks to all data providers listed in Table 4.

References

Aspmo, K., Gauchard, P. A., Steffen, A., Temme, C., Berg, T., Bahlmann, E., Banic, C., Dommergue, A., Ebinghaus, R., Ferrari, C., Pirrone, N., Sprovieri, F., and Wibetoe, G.: Measurements of atmospheric mercury species during an international study of mercury depletion events at Ny-Alesund, Svalbard, spring 2003. How reproducible are our present methods?, Atmos. Environ., 39, 7607–7619, doi:10.1016/j.atmosenv.2005.07.065, 2005.

Aucott, M. L., Caldarelli, A. D., Zsolway, R. R., Pietarinen, C. B., and England, R.: Ambient elemental, reactive gaseous, and particle-bound mercury concentrations in New Jersey, US: measurements and associations with wind direction, Environ. Monit. Assess., 158, 295–306, doi:10.1007/s10661-008-0583-0, 2009.

Author Collective: Findings and recommendations from a workshop on "reducing the uncertainty in 2 measurements of atmospheric Hg" held at the University of Washington 23–25 October 2008, Report of the Uncertainty Workshop, 1–17, 2009.

Bloom, N. and Fitzgerald, W. F.: Determination of volatile mercury species at the picogram level by low-temperature gas-chromatography with cold-vapor atomic fluorescence detection, Anal. Chim. Acta, 208, 151–161, doi:10.1016/S0003-2670(00)80743-6, 1988.

ACPD

12, 17245–17293, 2012

Brooks, S., Luke, W., Cohen, M., Kelly, P., Lefer, B., and Rappenglueck, B.: Mercury species measured atop the moody tower tramp site, Houston, Texas, Atmos. Environ., 44, 4045–4055, doi:10.1016/j.atmosenv.2009.02.009, 2010.

Brown, R. J. C., Brown, A. S., Yardley, R. E., Corns, W. T., and Stockwell, P. B.: A practical uncertainty budget for ambient mercury vapour measurement, Atmos. Environ., 42, 2504–2517, doi:10.1016/j.atmosenv.2007.12.012, 2008.

Bullock, O. R. and Brehme, K. A.: Atmospheric mercury simulation using the CMAQ model: formulation description and analysis of wet deposition results, Atmos. Environ., 36, 2135–2146, doi:10.1016/S1352-2310(02)00220-0, 2002.

Bullock, O. R., Atkinson, D., Braverman, T., Civerolo, K., Dastoor, A., Davignon, D., Ku, J.-Y., Lohman, K., Myers, T. C., Park, R. J., Seigneur, C., Selin, N. E., Sistla, G., and Vijayaraghavan, K.: An analysis of simulated wet deposition of mercury from the North American mercury model intercomparison study, J. Geophys. Res.-Atmos., 114, D08301, doi:10.1029/2008JD011224, 2009.

Caldwell, C. A., Swartzendruber, P., and Prestbo, E.: Concentration and dry deposition of mercury species in arid South Central New Mexico (2001–2002), Environ. Sci. Technol., 40, 7535–7540, doi:10.1021/es0609957, 2006.

Choi, H. D., Sharac, T. J., and Holsen, T. M.: Mercury deposition in the Adirondacks: a comparison between precipitation and throughfall, Atmos. Environ., 42, 1818–1827, doi:10.1016/j.atmosenv.2007.11.036, 2008.

Côté, J., Gravel, S., Méthot, A., Patoine, A., Roch, M., and Staniforth, A.: The operational CMC-MRB Global Environmental Multiscale (GEM) model, Part I: Design considerations and formulation. Mon. Wea. Rev., 126, 1373–1395, doi:10.1175/1520-0493(1998)126<1373:TOCMGE>2.0.CO;2, 1998a.

Côté, J., Desmarais, J.-G., Gravel, S., Méthot, A., Patoine, A., Roch, M., and Staniforth, A.: The operational CMC-MRB Global Environmental Multiscale (GEM) model, Part II: Results, Mon. Weather Rev., 126, 1397–1418, doi:10.1175/1520-0493(1998)126<1397:TOCMGE>2.0.CO;2, 1998b.

Dastoor, A. P., and Larocque, Y.: Global circulation of atmospheric mercury: a modelling study, Atmos. Environ., 38, 147–161, doi:10.1016/j.atmosenv.2003.08.037, 2004.

Dastoor, A. P., Davignon, D., Theys, N., Van Roozendael, M., Steffen, A., and Ariya, P. A.: Modeling dynamic exchange of gaseous elemental mercury at polar sunrise, Environ. Sci. Technol., 42, 5183–5188, doi:10.1021/es800291w, 2008.

ACPD
12, 17245–17293, 2012

Donohoue, D. L., Bauer, D., Cossairt, B., and Hynes, A. J.: Temperature and pressure dependent rate coefficients for the reaction of hg with br and the reaction of Br with Br: a pulsed laser photolysis-pulsed laser induced fluorescence study, J. Phys. Chem. A, 110, 6623–6632, doi:10.1021/jp054688j, 2006.

Durnford, D., Dastoor, A., Figueras-Nieto, D., and Ryjkov, A.: Long range transport of mercury to the Arctic and across Canada, Atmos. Chem. Phys., 10, 6063–6086, doi:10.5194/acp-10-6063-2010, 2010.

Edgerton, E. S., Hartsell, B. E., and Jansen, J. J.: Mercury speciation in coal-fired power plant plumes observed at three surface sites in the Southeastern US, Environ. Sci. Technol., 40, 4563–4570, doi:10.1021/es0515607, 2006.

Engle, M. A., Tate, M. T., Krabbenhoft, D. P., Schauer, J. J., Kolker, A., Shanley, J. B., and Bothner, M. H.: Comparison of atmospheric mercury speciation and deposition at nine sites across Central and Eastern North America, J. Geophys. Res.-Atmos., 115, D18306. doi:10.1029/2010JD014064, 2010.

Fitzgerald, W. F.: Is mercury increasing in the atmosphere – the need for an atmospheric mercury network (AMNet), Water Air Soil Poll., 80, 245–254, doi:10.1007/BF01189674, 1995.

Fu, X. W., Feng, X. B., Zhu, W. Z., Zheng, W., Wang, S. F., and Lu, J. Y.: Total particulate and reactive gaseous mercury in ambient air on the eastern slope of the Mt. Gongga area, China, Appl. Geochem., 23, 408–418, doi:10.1016/j.apgeochem.2007.12.018, 2008.

Gabriel, M. C., Williamson, D. G., Brooks, S., and Lindberg, S.: Atmospheric speciation of Southeastern mercury in two contrasting US airsheds, Atmos. Environ., 39, 4947–4958, doi:10.1016/j.atmosenv.2005.05.003, 2005.

Goodsite, M. E., Plane, J. M. C., and Skov, H.: A theoretical study of the oxidation of Hg to HgBr in the troposphere, Environ. Sci. Technol., 38, 1772–1776, doi:10.1021/es034680s, 2004.

Hall, B.: The gas-phase oxidation of elemental mercury by ozone, Water Air Soil Poll., 80, 301–315, 1995.

Hall, B. D., Olson, M. L., Rutter, A. P., Frontiera, R. R., Krabbenhoft, D. P., Gross, D. S., Yuen, M., Rudolph, T. M., and Schauer, J. J.: Atmospheric mercury speciation in Yellowstone National Park, Sci. Total. Environ., 367, 354–366, doi:10.1016/j.scitotenv.2005.12.007, 2006.

Han, Y. J., Holsen, T. M., Lai, S. O., Hopke, P. K., Yi, S. M., Liu, W., Pagano, J., Falanga, L., Milligan, M., and Andolina, C.: Atmospheric gaseous mercury concentrations in New York state: relationships with meteorological data and other pollutants, Atmos. Environ., 38, 6431–6446, doi:10.1016/j.atmosenv.2004.07.031, 2004.

ACPD
12, 17245–17293, 2012

Helsel, D. R.: Less than obvious – statistical treatment of data below the detection limit, Environ. Sci. Technol., 24, 1766–1774, 1990.
Helsel, D. R.: More than obvious: better methods for interpreting nondetect data, Environ. Sci. Technol., 39, 419A–423A, 2005.
Holmes, C. D., Jacob, D. J., Corbitt, E. S., Mao, J., Yang, X., Talbot, R., and Slemr, F.: Accurate global potential energy surface and reaction dynamics for the ground state of $HgBr_2$, J. Phys. Chem. A, 109, 8765–8773, doi:10.1021/jp053415l, 2009.
Holmes, C. D., Jacob, D. J., Corbitt, E. S., Mao, J., Yang, X., Talbot, R., and Slemr, F.: Global atmospheric model for mercury including oxidation by bromine atoms, Atmos. Chem. Phys., 10, 12037–12057, doi:10.5194/acp-10-12037-2010, 2010.
Hsi, H. C., Lee, H. H., Hwang, J. F., and Chen, W.: Mercury speciation and distribution in a 660-megawatt utility boiler in Taiwan firing bituminous coals, J. Air Waste Manage., 60, 514–522, doi:10.3155/1047-3289.60.5.514, 2010.
Huang, J. Y., Choi, H. D., Hopke, P. K., and Holsen, T. M.: Ambient mercury sources in Rochester, NY: results from principle components analysis (PCA) of mercury monitoring network data, Environ. Sci. Technol., 44, 8441–8445, doi:10.1021/es102744j, 2010.
Jaffe, D., Prestbo, E., Swartzendruber, P., Weiss-Penzias, P., Kato, S., Takami, A., Hatakeyama, S., and Kajji, Y.: Export of atmospheric mercury from Asia, Atmos. Environ., 39, 3029–3038, doi:10.1016/j.atmosenv.2005.01.030, 2005.
Justino, C. I. L., Rocha-Santos, T. A., and Duarte, A. C.: Sampling and characterization of nanoaerosols in different environments, TRAC-Trend. Anal. Chem., 30, 554–567, doi:10.1016/j.trac.2010.12.002, 2011.
Keeler, G., Glinsorn, G., and Pirrone, N.: Particulate mercury in the atmosphere – its significance, transport, transformation and sources, Water Air Soil Poll., 80, 159–168, 1995.
Kim, J. H., Park, J. M., Lee, S. B., Pudasainee, D., and Seo, Y. C.: Anthropogenic mercury emission inventory with emission factors and total emission in Korea, Atmos. Environ., 44, 2714–2721, doi:10.1016/j.atmosenv.2010.04.037, 2010.
Klockow, D., Siemens, V., and Larjava, K.: Application of diffusion separators for measurement of metal emissions, VDI Bericht, 838, 389–400, 1990.
Kocman, D. and Horvat, M.: A laboratory based experimental study of mercury emission from contaminated soils in the River Idrijca catchment, Atmos. Chem. Phys., 10, 1417–1426, doi:10.5194/acp-10-1417-2010, 2010.

ACPD
12, 17245–17293, 2012

Kolker, A., Olson, M. L., Krabbenhoft, D. P., Tate, M. T., and Engle, M. A.: Patterns of mercury dispersion from local and regional emission sources, rural Central Wisconsin, USA, Atmos. Chem. Phys., 10, 4467–4476, doi:10.5194/acp-10-4467-2010, 2010.

Landis, M. S., Stevens, R. K., Schaedlich, F., and Prestbo, E. M.: Development and characterization of an annular denuder methodology for the measurement of divalent inorganic reactive gaseous mercury in ambient air, Environ. Sci. Tech., 36, 3000–3009, doi:10.1021/es015887t, 2002.

Li, J., Sommar, J., Wangberg, I., Lindqvist, O., and Wei, S. Q.: Short-time variation of mercury speciation in the urban of Goteborg during GOTE-2005, Atmos. Environ., 42, 8382–8388, doi:10.1016/j.atmosenv.2008.08.007, 2008.

Lindberg, S. E. and Stratton, W. J.: Atmospheric mercury speciation: concentrations and behavior of reactive gaseous mercury in ambient air, Environ. Sci. Technol., 32, 49–57, doi:10.1021/es970546u, 1998.

Lindberg, S. E., Hanson, P. J., Meyers, T. P., and Kim, K. H.: Air/surface exchange of mercury vapor over forests – the need for a reassessment of continental biogenic emissions, Atmos. Environ., 32, 895–908, doi:10.1016/S1352-2310(97)00173-8, 1998.

Lindberg, S. E., Brooks, S., Lin, C. J., Scott, K. J., Landis, M. S., Stevens, R. K., Goodsite, M., and Richter, A.: Dynamic oxidation of gaseous mercury in the arctic troposphere at polar sunrise, Environ. Sci. Tech., 36, 1245–1256, doi:10.1021/es0111941, 2002.

Lindberg, S., Bullock, R., Ebinghaus, R., Engstrom, D., Feng, X. B., Fitzgerald, W., Pirrone, N., Prestbo, E., and Seigneur, C.: A synthesis of progress and uncertainties in attributing the sources of mercury in deposition, Ambio, 36, 19–32, doi:10.1579/0044-7447(2007)36[19:ASOPAU]2.0.CO;2, 2007.

Liu, B., Keeler, G. J., Dvonch, J. T., Barres, J. A., Lynam, M. M., Marsik, F. J., and Morgan, J. T.: Temporal variability of mercury speciation in urban air, Atmos. Environ., 41, 1911–1923, doi:10.1016/j.atmosenv.2006.10.063, 2007.

Liu, B., Keeler, G. J., Dvonch, J. T., Barres, J. A., Lynam, M. M., Marsik, F. J., and Morgan, J. T.: Urban-rural differences in atmospheric mercury speciation, Atmos. Environ., 44, 2013–2023, doi:10.1016/j.atmosenv.2010.02.012, 2010.

Liu, N., Qiu, G. G., Landis, M. S., Feng, X. B., Fu, X. W., and Shang, L. H.: Atmospheric mercury species measured in Guiyang, Guizhou province, Southwest China, Atmos. Res., 100, 93–102, doi:10.1016/j.atmosres.2011.01.002, 2011.

ACPD
12, 17245–17293, 2012

Lohman, K., Seigneur, C., Edgerton, E., and Jansen, J.: Modeling mercury in power plant plumes, Environ. Sci. Technol., 40, 3848–3854, doi:10.1021/es051556v, 2006.
Lyman, S. N. and Gustin, M. S.: Determinants of atmospheric mercury concentrations in Reno, Nevada, USA, Sci. Total Environ., 408, 431–438, doi:10.1016/j.scitotenv.2009.09.045, 2009.
Lyman, S. N., Jaffe, D. A., and Gustin, M. S., Release of mercury halides from KCl denuders in the presence of ozone. Atmos. Chem. Phys. 10, 8197–8204, doi:10.5194/acp-10-8197-2010, 2010.
Malcolm, E. G. and Keeler, G. J.: Evidence for a sampling artifact for particulate-phase mercury in the marine atmosphere, Atmos. Environ., 41, 3352–3359, doi:10.1016/j.atmosenv.2006.12.024, 2007.
Manolopoulos, H., Schauer, J. J., Purcell, M. D., Rudolph, T. M., Olson, M. L., Rodger, B., and Krabbenhoft, D. P.: Local and regional factors affecting atmospheric mercury speciation at a remote location, J. Environ. Eng. Sci., 6, 491–501, doi:10.1139/S07-005, 2007.
Mason, R. P.: Mercury emissions from natural processes and their importance in the global mercury cycle, in: Mercury Fate and Transport in the Global Atmosphere, edited by: Mason, R. and Pirrone, N., Springer US, Boston, MA, doi:10.1007/978-0-387-93958-2, 173–191, 2009.
Maynard, A. D. and Aitken, R. J.: Assessing exposure to airborne nanomaterials: current abilities and future requirements, Nanotoxicology, 1, 26–41, doi:10.1080/17435390701314720, 2007.
Munthe, J., Xiao, Z. F., and Lindqvist, O.: The aqueous reduction of divalent mercury by sulfite, Water Air Soil Poll., 56, 621–630, 1991.
Munthe, J., Wangberg, I., Pirrone, N., Iverfeldt, A., Ferrara, R., Ebinghaus, R., Feng, X., Gardfeldt, K., Keeler, G., Lanzillotta, E., Lindberg, S. E., Lu, J., Mamane, Y., Prestbo, E., Schmolke, S., Schroeder, W. H., Sommar, J., Sprovieri, F., Stevens, R. K., Stratton, W., Tuncel, G., and Urba, A.: Intercomparison of methods for sampling and analysis of atmospheric mercury species, Atmos. Environ., 35, 3007–3017, 2001.
Munthe, J., Wangberg, I., Iverfeldt, A., Lindqvist, O., Stromberg, D., Sommar, J., Gardfeldt, K., Petersen, G., Ebinghaus, R., Prestbo, E., Larjava, K., and Siemens, V.: Distribution of atmospheric mercury species in Northern Europe: final results from the moe project, Atmos. Environ., 37, S9–S20, doi:10.1016/S1352-2310(03)00235-8, 2003.
NAD Program: Atmospheric mercury network site operations manual, version 1.0, Operations Manual, 1–36, available at: http://nadp.isws.illinois.edu, last access: 18 June 2012, 2011.

ACPD
12, 17245–17293, 2012

Niksa, S., Naik, C. V., Berry, M. S., and Monroe, L.: Interpreting enhanced Hg oxidation with br addition at plant miller, Fuel Process Technol., 90, 1372–1377, doi:10.1016/j.fuproc.2009.05.022, 2009.

Pacyna, E. G., Pacyna, J. M., Sundseth, K., Munthe, J., Kindbom, K., Wilson, S., Steenhuisen, F., and Maxson, P.: Global emission of mercury to the atmosphere from anthropogenic sources in 2005 and projections to 2020, Atmos. Environ., 44, 2487–2499, doi:10.1016/j.atmosenv.2009.06.009, 2010.

Pehkonen, S. O. and Lin, C. J.: Aqueous photochemistry of mercury with organic acids, J. Air Waste Manage. Assoc., 48, 144–150, 1998.

Peterson, S. A., Ralston, N. V. C., Peck, D. V., Van, S. J., Robertson, J. D., Spate, V. L., and Morris, J. S.: How might selenium moderate the toxic effects of mercury in stream fish of the Western US?, Environ. Sci. Technol., 43, 3919–3925, doi:10.1021/es803203g, 2009.

Poissant, L., Pilote, M., Xu, X. H., Zhang, H., and Beauvais, C.: Atmospheric mercury speciation and deposition in the bay St. Francois wetlands, J. Geophys. Res.-Atmos., 109, D11301, doi:10.1029/2003JD004364, 2004.

Poissant, L., Pilote, M., Beauvais, C., Constant, P., and Zhang, H. H.: A year of continuous measurements of three atmospheric mercury species (GEM, RGM and Hg-p) in Southern Quebec, Canada, Atmos. Environ., 39, 1275–1287, doi:10.1016/j.atmosenv.2004.11.007, 2005.

Prestbo, E. M. and Gay, D. A.: Wet deposition of mercury in the US and Canada, 1996–2005: results and analysis of the NADP mercury deposition network (MDN), Atmos. Environ., 43, 4223–4233, doi:10.1016/j.atmosenv.2009.05.028, 2009.

Rothenberg, S. E., Mckee, L., Gilbreath, A., Yee, D., Connor, M., and Fu, X. W.: Evidence for short-range transport of atmospheric mercury to a rural, inland site, Atmos. Environ., 44, 1263–1273, doi:10.1016/j.atmosenv.2009.12.032, 2010a.

Rothenberg, S. E., Mckee, L., Gilbreath, A., Yee, D., Connor, M., and Fu, X. W.: Wet deposition of mercury within the vicinity of a cement plant before and during cement plant maintenance, Atmos. Environ., 44, 1255–1262, doi:10.1016/j.atmosenv.2009.12.033, 2010b.

Rutter, A. P. and Schauer, J. J.: The impact of aerosol composition on the particle to gas partitioning of reactive mercury, Environ. Sci. Technol., 41, 3934–3939, doi:10.1021/es062439i, 2007.

Rutter, A. P., Snyder, D. C., Stone, E. A., Schauer, J. J., Gonzalez-Abraham, R., Molina, L. T., Márquez, C., Cárdenas, B., and de Foy, B.: In situ measurements of speciated atmospheric

ACPD
12, 17245–17293, 2012

mercury and the identification of source regions in the Mexico City Metropolitan Area, Atmos. Chem. Phys., 9, 207–220, doi:10.5194/acp-9-207-2009, 2009.
Ryaboshapko, A., Bullock, O. R., Christensen, J., Cohen, M., Dastoor, A., Ilyin, I., Petersen, G., Syrakov, D., Artz, R. S., Davignon, D., Draxler, R. R., and Munthe, J.: Intercomparison study of atmospheric mercury models: 1. Comparison of models with short-term measurements, Sci. Total Environ., 376, 228–240, doi:10.1016/j.scitotenv.2007.01.072, 2007a.
Ryaboshapko, A., Bullock, O. R., Christensen, J., Cohen, M., Dastoor, A., Ilyin, I., Petersen, G., Syrakov, D., Travnikov, O., Artz, R. S., Davignon, D., Draxler, R. R., Munthe, J., and Pacyna, J.: Intercomparison study of atmospheric mercury models: 2. Modelling results vs. long-term observations and comparison of country deposition budgets, Sci. Total Environ., 377, 319–333, doi:10.1016/j.scitotenv.2007.01.071, 2007b.
Sanei, H., Outridge, P. M., Goodarzi, F., Wang, F., Armstrong, D., Warren, K., and Fishback, L.: Wet deposition mercury fluxes in the Canadian sub-arctic and Southern Alberta, measured using an automated precipitation collector adapted to cold regions, Atmos. Environ., 44, 1672–1681, doi:10.1016/j.atmosenv.2010.01.030, 2010.
Schroeder, W. H. and Munthe, J.: Atmospheric mercury – an overview, Atmos. Environ., 32, 809–822, 1998.
Seigneur, C., Vijayaraghavan, K., Lohman, K., Karamchandani, P., and Scott, C.: Modeling the atmospheric fate and transport of mercury over North America: power plant emission scenarios, Fuel Process Technol., 85, 441–450, doi:10.1016/j.fuproc.2003.11.001, 2004.
Selin, N. E.: Global biogeochemical cycling of mercury: a review, Annu. Rev. Environ. Resour., 34, 43–63, doi:10.1146/annurev.environ.051308.084314, 2009.
Selin, N. E. and Jacob, D. J.: Seasonal and spatial patterns of mercury wet deposition in the United States: constraints on the contribution from North American anthropogenic sources, Atmos. Environ., 42, 5193–5204, doi:10.1016/j.atmosenv.2008.02.069, 2008.
Shah, P., Strezov, V., and Nelson, P. F.: Speciation of mercury in coal-fired power station flue gas, Energ. Fuel, 24, 205–212, doi:10.1021/ef900557p, 2010.
Sheu, G. R., Mason, R. P., and Lawson, N. M.: Speciation and distribution of atmospheric mercury over the Northern Chesapeake Bay, in: Chemicals in the Environment: Fate, Impacts, and Remediation, edited by: Lipnick, R. L., American Chemical Society Publication, 223–242, doi:10.1021/bk-2002–0806.ch012, 2002.
Sheu, G. R., Lin, N. H., Wang, J. L., Lee, C. T., Yang, C. F. O., and Wang, S. H.: Temporal distribution and potential sources of atmospheric mercury measured at

ACPD
12, 17245–17293, 2012

a high-elevation background station in Taiwan, Atmos. Environ., 44, 2393–2400, doi:10.1016/j.atmosenv.2010.04.009, 2010.
Sigler, J. M., Mao, H., and Talbot, R.: Gaseous elemental and reactive mercury in Southern New Hampshire, Atmos. Chem. Phys., 9, 1929–1942, doi:10.5194/acp-9-1929-2009, 2009.
Slemr, F., Ebinghaus, R., Brenninkmeijer, C. A. M., Hermann, M., Kock, H. H., Martinsson, B. G., Schuck, T., Sprung, D., van Velthoven, P., Zahn, A., and Ziereis, H.: Gaseous mercury distribution in the upper troposphere and lower stratosphere observed onboard the CARIBIC passenger aircraft, Atmos. Chem. Phys., 9, 1957–1969, doi:10.5194/acp-9-1957-2009, 2009.
Sommar, J., Gårdfeldt, K., Strömberg, D., and Feng, X.: A kinetic study of the gas-phase reaction between the hydroxyl radical and atomic mercury, Atmos. Environ., 35, 3049–3054, doi:10.1016/S1352-2310(01)00108-X, 2001.
Sommar, J., Andersson, M. E., and Jacobi, H.-W.: Circumpolar measurements of speciated mercury, ozone and carbon monoxide in the boundary layer of the Arctic Ocean, Atmos. Chem. Phys., 10, 5031–5045, doi:10.5194/acp-10-5031-2010, 2010.
Song, X. J., Cheng, I., and Lu, J.: Annual atmospheric mercury species in downtown Toronto, Canada, J. Environ. Monitor., 11, 660–669, doi:10.1039/b815435j, 2009.
Steen, A. O., Berg, T., Dastoor, A. P., Durnford, D. A., Hole, L. R., and Pfaffhuber-Aspmo, K.: Dynamic exchange of gaseous elemental mercury during polar night and day, Atmos. Environ., 43, 5604–5610, doi:10.1016/j.atmosenv.2009.07.069, 2009.
Steffen, A., Scherz, T., Olson, M., Gay, D., and Blanchard, P.: A comparison of data quality control protocols for atmospheric mercury speciation measurements, J. Environ. Monit., 14, 752–765, doi:10.1039/c2em10735j, 2012.
Swartzendruber, P. C., Jaffe, D. A., Prestbo, E. M., Weiss-Penzias, P., Selin, N. E., Park, R., Jacob, D. J., Strode, S., and Jaegle, L.: Observations of reactive gaseous mercury in the free troposphere at the Mount Bachelor observatory, J. Geophys. Res.-Atmos., 111, D24302, doi:10.1029/2006JD007415, 2006.
Swartzendruber, P. C., Jaffe, D. A., and Finley, B.: Improved fluorescence peak integration in the Tekran 2537 for applications with sub-optimal sample loadings, Atmos. Environ., 43, 3648–3651, doi:10.1016/j.atmosenv.2009.02.063, 2009.
Temme, C., Blanchard, P., Steffen, A., Banic, C., Beauchamp, S., Poissant, L., Tordon, R., and Wiens, B.: Trend, seasonal and multivariate analysis study of total gaseous mercury data from the Canadian atmospheric mercury measurement network (CAMNet), Atmos. Environ., 41, 5423–5441, doi:10.1016/j.atmosenv.2007.02.021, 2007.

ACPD
12, 17245–17293, 2012

Van Loon, L. L., Mader, E., and Scott, S. L.: Reduction of the aqueous mercuric ion by sulfite: UV spectrum of $HgSO_3$ and its intramolecular redox reaction, J. Phys. Chem. A, 104, 1621–1626, doi:10.1021/jp994268s, 2000.

Van Loon, L. L., Mader, E. A., and Scott, S. L.: Sulfite stabilization and reduction of the aqueous mercuric ion: kinetic determination of sequential formation constants, J. Phys. Chem. A, 105, 3190–3195, doi:10.1021/jp003803h, 2001.

Vijayaraghavan, K., Karamchandani, P., Seigneur, C., Balmori, R., and Chen, S.-Y.: Plume-in-grid modeling of atmospheric mercury, J. Geophys. Res., 113, D24305, doi:10.1029/2008JD010580, 2008.

Wan, Q., Feng, X. B., Lu, J., Zheng, W., Song, X. J., Li, P., Han, S. J., and Xu, H.: Atmospheric mercury in Changbai mountain area, Northeastern China II. The distribution of reactive gaseous mercury and particulate mercury and mercury deposition fluxes, Environ. Res., 109, 721–727, doi:10.1016/j.envres.2009.05.006, 2009a.

Wan, Q., Feng, X. B., Lu, J. L., Zheng, W., Song, X. J., Han, S. J., and Xu, H.: Atmospheric mercury in Changbai Mountain area, Northeastern China. I. The seasonal distribution pattern of total gaseous mercury and its potential sources, Environ. Res., 109, 201–206, doi:10.1016/j.envres.2008.12.001, 2009b.

Wang, S. X., Zhang, L., Li, G. H., Wu, Y., Hao, J. M., Pirrone, N., Sprovieri, F., and Ancora, M. P.: Mercury emission and speciation of coal-fired power plants in China, Atmos. Chem. Phys., 10, 1183–1192, doi:10.5194/acp-10-1183-2010, 2010.

Wang, Y. J., Duan, Y. F., Yang, L. G., Zhao, C. S., and Xu, Y. Q.: Mercury speciation and emission from the coal-fired power plant filled with flue gas desulfurization equipment, Can. J. Chem. Eng., 88, 867–873, doi:10.1002/cjce.20331, 2010.

Weiss-Penzias, P., Jaffe, D. A., McClintick, A., Prestbo, E. M., and Landis, M. S.: Gaseous elemental mercury in the marine boundary layer: Evidence for rapid removal in anthropogenic pollution, Environ. Sci. Technol., 37, 3755–3763, doi:10.1021/es0341081, 2003a.

Weiss-Penzias, P., Jaffe, D. A., McClintick, A., Prestbo, E. M., and Landis, M. S.: Gaseous elemental mercury in the marine boundary layer: evidence for rapid removal in anthropogenic pollution, Environ. Sci. Tech., 37, 3755–3763, doi:10.1021/es0341081, 2003b.

Weiss-Penzias, P., Jaffe, D., Swartzendruber, P., Hafner, W., Chand, D., and Prestbo, E.: Quantifying asian and biomass burning sources of mercury using the Hg/CO ratio in pollution plumes observed at the mount bachelor observatory, Atmos. Environ., 41, 4366–4379, doi:10.1016/j.atmosenv.2007.01.058, 2007.

ACPD
12, 17245–17293, 2012

Weiss-Penzias, P., Gustin, M. S., and Lyman, S. N.: Observations of speciated atmospheric mercury at three sites in nevada: evidence for a free tropospheric source of reactive gaseous mercury, J. Geophys. Res.-Atmos., 114, D14302, doi:10.1029/2008JD011607, 2009.

Wu, C. L., Cao, Y., Dong, Z., Cheng, C., Li, H., and Pan, W.: Evaluation of mercury speciation and removal through air pollution control devices of a 190 MW boiler, J. Environ. Sci., 22, 277–282, doi:10.1016/S1001-0742(09)60105-4, 2010a.

Wu, Y., Streets, D. G., Wang, S. X., and Hao, J. M.: Uncertainties in estimating mercury emissions from coal-fired power plants in China, Atmos. Chem. Phys., 10, 2937–2946, doi:10.5194/acp-10-2937-2010, 2010b.

Xiao, Z. F., Stromberg, D., and Lindqvist, O.: Influence of humic substances on photolysis of divalent mercury in aqueous solution, Water Air Soil Poll., 80, 789–798, doi:10.1007/BF01189730, 1995.

Yatavelli, R. L. N., Fahrni, J. K., Kim, M., Crist, K. C., Vickers, C. D., Winter, S. E., and Connell, D. P.: Mercury, $PM_{2.5}$ and gaseous co-pollutants in the Ohio River valley region: preliminary results from the Athens supersite, Atmos. Environ., 40, 6650–6665, doi:10.1016/j.atmosenv.2006.05.072, 2006.

Zhang, L.: A size-segregated particle dry deposition scheme for an atmospheric aerosol module, Atmos. Environ., 35, 549–560, doi:10.1016/S1352-2310(00)00326-5, 2001.

Zhang, L., Brook, J. R., and Vet, R.: A revised parameterization for gaseous dry deposition in air-quality models, Atmos. Chem. Phys., 3, 1777–1804, doi:10.5194/acpd-3-1777-2003, 2003.

Zhang, L. M., Wright, L. P., and Blanchard, P.: A review of current knowledge concerning dry deposition of atmospheric mercury, Atmos. Environ., 43, 5853–5864, 2009.

Zhang, L., Blanchard, P., Johnson, D., Dastoor, A., Ryzhkov, A., Lin, C. J., Vijayaraghavan, K., Gay, D., Holsen, T. M., Huang, J., Graydon, J. A., St Louis, V. L., Castro, M. S., Miller, E. K., Marsik, F., Lu, J., Poissant, L., Pilote, M., and Zhang, K. M.: Assessment of modeled mercury dry deposition over the Great Lakes region, Environ. Poll., 161, 272–283, doi:10.1016/j.envpol.2011.06.003, 2012a.

Zhang, Y., Jaeglé, L., van Donkelaar, A., Martin, R. V., Holmes, C. D., Amos, H. M., Wang, Q., Talbot, R., Artz, R., Brooks, S., Luke, W., Holsen, T. M., Felton, D., Miller, E. K., Perry, K. D., Schmeltz, D., Steffen, A., Tordon, R., Weiss-Penzias, P., and Zsolway, R.: Nested-grid simulation of mercury over North America, Atmos. Chem. Phys. Discuss., 12, 2603–2646, doi:10.5194/acpd-12-2603-2012, 2012b.

ACPD
12, 17245–17293, 2012

Table 1. Summary of literature data of Hg^{2+} and Hg_p measurements published from 2002 to 2010. All concentrations in pg m^{-3}. Uncertainties, where available, and significant figures are as reported by authors. Hg^{2+}/Hg_p ratios were calculated from reported speciation data. "~" indicates Hg^{2+}/Hg_p estimations based on concentration ranges reported by original authors.

Hg^{2+}	Hg_p	Hg^{2+}/Hg_p	Approximate location	Reference
8 ± 13	8 ± 25	1.0	Ny-Ålesund, Svalbard	Steen et al. (2009)
3.2	1.0	3.2	Arctic	Sommar et al. (2010)
19	47	0.40	Indrija, Slovenia	Kocman and Horvat (2010)
5.17	9.15	0.57	Devil's Lake, WI	Engle et al. (2010)
2.0	2.2	0.91	Lostwood Refuge, ND	Engle et al. (2010)
1.8	4.6	0.39	Shenandoah Park, VA	Engle et al. (2010)
37.5	25.4	1.47	East St. Louis, IL	Engle et al. (2010)
10.1	11.8	0.86	Milwaukee, WI	Engle et al. (2010)
3.8	2.8	1.36	Weeks Bay, AL	Engle et al. (2010)
3.3	2.3	1.43	Charleston, SC	Engle et al. (2010)
2.7	4.0	0.68	Cape Cod, MA	Engle et al. (2010)
1.5	1.2	1.3	Puerto Rico, PR	Engle et al. (2010)
4.08	6.57	0.62	Rochester, NY	Huang et al. (2010)
0.6–0.8	2.6–5.0	0.18	Central Wisconsin	Kolker et al. (2010)
0–60	0–80	~ 0.75	Houston, TX	Brooks et al. (2010)
15.5 ± 54.9	18.1 ± 61.0	0.86	Detroit, MI	Liu et al. (2010)
3.8 ± 6.6	6.1 ± 5.5	0.62	Dexter, MI	Liu et al. (2010)
12.1	2.3	5.26	Mt. Front Lulin, Taiwan	Sheu et al. (2010)
25.2 ± 52.8	80.8 ± 283	0.31	Cement plant, CA	Rothenberg et al. (2010b)
2.58 ± 1.28	3.17 ± 3.20	0.81	Moffet, CA	Rothenberg et al. (2010a)
14.5 ± 30.2	7.99 ± 6.74	1.81	Calero, CA	Rothenberg et al. (2010a)
8.93 ± 0.31	8.21 ± 0.39	1.09	Elizabeth, NJ	Aucott et al. (2009)
10.73 ± 0.45	6.04 ± 0.30	1.78	New Brunswick, NJ	Aucott et al. (2009)
14.2 ± 13.2	21.5 ± 16.4	0.66	Toronto, ON	Song et al. (2009)
26, 45, 86	6, 5, 10	4.3, 9, 8.6	Nevada	Weiss-Penzias et al. (2009)
62 ± 64	187 ± 300	0.33	Mexico City	Rutter et al. (2009)
65	77	0.84	Mt. Changbai, NE China	Wan et al. (2009) Wan et al. (2009a)
26 ± 35	9 ± 10	2.9	Reno, NV	Peterson et al. (2009)
18 ± 22	7 ± 7	2.6	Reno, NV	Lyman and Gustin, 2009
6.8	1.52	4.5	New Mexico	Caldwell et al. (2006)
1.8 ± 2.2	3.2 ± 3.7	0.56	Newcomb, NY	Choi et al. (2008)
2.53 ± 4.09	12.50 ± 5.88	0.20	Goteborg, Sweden	Li et al. (2008)
6.2	30.7	0.20	Mt. Gongga, China	Fu et al. (2008)
39–60	4.4	~ 10	Mt. Bachelor, USA	Weiss-Penzias et al. (2007)
0–5	0–30	~ 0.17	Yellowstone National Park	Hall et al. (2006)
3.8 ± 8.9	8.6 ± 8.3	0.44	Devil's Lake, WI	Manolopoulos et al. (2007)
17.7 ± 28.9	20.8 ± 30.0	0.84	Detroit, MI	Liu et al. (2007)
43	5.2	8.3	Mt. Bachelor	Swartzendruber et al. (2006)
13.6 ± 20.4	16.4 ± 19.5	0.83	Tuscaloosa, AL	Gabriel et al. (2005)
13.6 ± 7.4	9.73 ± 6.9	1.40	Cove Mountain, TN	Gabriel et al. (2005)
3 ± 11	26 ± 54	0.12	St. Anicet, QC	Poissant et al. (2005)
5 ± 5	6 ± 7	~ 1	Point Petre, ON	Han et al. (2004)
3.63	6.44	0.56	St. Francois wetlands, QC	Poissant et al. (2004)
18	25	0.72	Neuglobsow, Germany	Munthe et al. (2003)
26	23	1.1	Zingst, Germany	Munthe et al. (2003)
14	4	3.5	Rörvik, Sweden	Munthe et al. (2003)
10	5	2.0	Aspvreten, Sweden	Munthe et al. (2003)
18	2	9.0	Mace Head, Ireland	Munthe et al. (2003)
0–2.7	0–2.9	~ 1	Cheeka Peak	Weiss-Penzias et al. (2003a)
21 ± 22	42 ± 50	0.5	Stillpond, MD	Sheu et al. (2002)
89 ± 150	74 ± 197	1.20	Baltimore, MD	Sheu et al. (2002)

ACPD
12, 17245–17293, 2012

Table 2. Description of model runs and most important parameters that were used in this study. The "Base" experiment corresponds to estimates used in Zhang et al. (2012a).

Experiment	Hg^0:Hg^{2+}:Hg_p	Oxidant	Remarks
Base	50:40:10	O_3; std rate	Base run
NoEmit	–	O_3; std rate	No anthropogenic Hg^{2+} and Hg_p emissions
NoChem	50:40:10	O_3; std rate	No oxidation processes
Ex-ox1.5-CFPP	90:5:5	O_3; 1.5× rate	Emission adjustment for coal-fired power plants (CFPP) only
Ex-ox1	90:8:2	O_3; std rate	
Ex-ox2	90:8:2	O_3; 2× rate	
Ex-ox2-HiHgp	90:8:2	O_3; 2× rate	Hg^{2+} : Hg_p ratio 0.75 ⇒ 0.25
Ex-oxOH	90:8:2	OH	OH oxidation only

ACPD
12, 17245–17293, 2012

Table 3. Measurement details and limits of detection for Hg^{2+} and Hg_p (all CVAFS; Tekran 2537A/1130/1135) at selected stations used for comparison with model results in Zhang et al. (2012a). Method performance data and parameters as cited. MDL: method detection limit.

Identifier/site	MDL ($pg\,m^{-3}$)	Reference	Remarks
OH02/Athens	<1 (Hg^{2+} and Hg_p)	Yatavelli et al. (2006)	AMNet site 1 h Hg^{2+} and Hg_p sampling
NJ05/Brigantine	1.0 (Species not given)	Aucott et al. (2009)	AMNet site 1 h Hg^{2+} and Hg_p sampling
NJ30/Chester	1.0 (Species not given)	Aucott et al. (2009)	AMNet site 1 h Hg^{2+} and Hg_p sampling
NJ54/Elizabeth	1.0 (Species not given)	Aucott et al. (2009)	AMNet site 1 h Hg^{2+} and Hg_p sampling
ON18/ Experimental Lakes Area	NA	Eckley (2011), Zhang (2011) both personal communication	Environment Canada site 3 h Hg^{2+} and Hg_p sampling
NY20/Huntington	0.46 (Hg^{2+}) 1.10 (Hg_p)	Huang et al. (2010)	AMNet site 2 h Hg^{2+} and Hg_p sampling Assuming same setup as Rochester
NJ30/New Brunswick	1.0 (Species not given)	Aucott et al. (2009)	AMNet site 1 h Hg^{2+} and Hg_p sampling
NY43/Rochester	0.46 (Hg^{2+}) 1.10 (Hg_p)	Huang et al. (2010)	AMNet site 2 h Hg^{2+} and Hg_p sampling
PQ04/St-Anicet	3.75 (Species not given)	Poissant et al. (2005)	Environment Canada site 1 h Hg^{2+} and Hg_p sampling
NH06/Thompson Farm	0.1 (Hg^{2+})	Sigler et al. (2009)	AMNet 2 h Hg^{2+} sampling
TORO/Toronto	4 (Hg^{2+} and Hg_p)	Song et al. (2009)	Ryerson University 1 h Hg^{2+} and Hg_p sampling
Laboratory study	6.2/3.1 (Hg^{2+}); 1-h/2-h sampling	Landis et al. (2002)	Characterisation of denuder method

ACPD
12, 17245–17293, 2012

Table 4. Observation sites for data used in this study. Two site identifiers at the same location indicate co-located instrument data. Yearly means (pg m^{-3}) for multiple years are similar. Sites were classified as C = close (60–90 pg m^{-3}), and I = intermediate proximitiy to sources (30–60 pg m^{-3}) and F = far from sources (0–30 pg m^{-3}) according to model calculation results plotted in Fig. 5. PI and data providers as of October 2010.

Site ID	Location	Lat	Lon	Obs Years	PI/Data Provider	Yearly average	Site
AB14	Genesee, AB	53.3016	−114.201	2009	Jacques Whitford Axys Ltd.	Hg^{2+}: 7.11 Hg_p: 4.95	F
ALER	Alert, NU	82.5000	−62.3330	2002–2009	Steffen, EC	Hg^{2+}: 7.69–30.8 Hg_p: 4.95–47.2	F
HALI	Halifax, NS	44.6700	−63.6100	2010	Tordon, EC	Hg^{2+}: 2.99 Hg_p: 2.52	F
MD08	Piney Reservoir, MD	39.7053	−79.0122	2008–2009	Castro, MD State University	Hg^{2+}: 8.79–15.9 Hg_p: 1.81–6.43	I
MS12/ MS99	Grand Bay, MS	30.4294	−88.4277	2008–2009	Brooks/Luke, NOAA	Hg^{2+}: 7.52–9.94 Hg_p: 4.33–5.39	F
NH06	Thompson Farm, NH	43.1100	−70.9500	2009	University of NH	Hg^{2+}: 3.35 Hg_p: 2.46	F
NJ30	New Brunswick, NJ	40.4728	−74.4225	2005 and 2009	Zsolway, NJ State University	Hg^{2+}: 3.82–8.23 Hg_p: 7.04–14.8	C
NJ32	Chester, NJ	40.7876	−74.6763	2005 and 2009	Zsolway, NJ State University	Hg^{2+}: 6.38–10.2 Hg_p: 10.5–12.1	C
NJ54	Elizabeth, NJ	40.6414	−74.2084	2005	Zsolway, NJ State University	Hg^{2+}: 11.0 Hg_p: 11.4	C
NS01	Kejimkujik, NS	44.4336	−65.2060	2009	Tordon/Steffen, EC	Hg^{2+}: 0.474 Hg_p: 5.72	F
NY06	Bronx, NY	40.8680	−73.8782	2009	Felton, NY State University	Hg^{2+}: 14.3 Hg_p: 16.1	F
NY20	Huntington Forest, NY	43.9731	−74.2231	2008–2009	Holsen, Clarkson University	Hg^{2+}: 0.907–1.62 Hg_p: 1.83–6.04	F
NY43/ NY95	Rochester, NY	43.1544	−77.6160	2008–2009	NY43: Holsen, Clarkson University NY 95: Felton, NY State University	Hg^{2+}: 7.40–10.0 Hg_p: 10.0–16.1	F
OH02	Athens, OH	39.3000	−82.1167	2008–2009	Crist/Conley, Ohio University	Hg^{2+}: 12.1–16.2 Hg_p: 7.82–9.57	I
OK99	Stilwell, OK	35.7514	−94.6717	2009	Callison/Scrapper, Cherokee Nation	Hg^{2+}: 2.93 Hg_p: 4.06	F
ON18	Experimental Lakes Area, ON	49.6639	−93.7211	2005–2006 and 2009	Eckley, EC	Hg^{2+}: 0.376–1.33 Hg_p: 3.23–5.26	F
PQ04	St. Anicet, QC	45.1167	−74.2830	2003, 2005 and 2009	Poissant, EC	Hg^{2+}: 3.21–4.99 Hg_p: 12.8–25.8	F
TORO	Toronto, ON	43.6700	−79.4000	2004	Lu, Ryerson University	Hg^{2+}: 14.5 Hg_p: 22.1	F
UT97	Salt Lake City, UT	40.7118	−111.961	2009	Olson, Utah State University	Hg^{2+}: 23.5 Hg_p: 15.5	C
VT99	Underhill, VT	44.5283	−72.8689	2008	Miller, Ecosystems Research	Hg^{2+}: 4.12 Hg_p: 13.4	F
WOOD	Woods Hole, MA	41.5267	−70.6631	2008	Engle, USGS	Hg^{2+}: 2.03 Hg_p: 2.91	F

ACPD
12, 17245–17293, 2012

Table 5. Quantitative uncertainty data for sampling, measurement (Tekran 2537A/1130/1135), emission and atmospheric chemistry-related parameters. Data is presented as calculated by the original authors.

#	Species	Process	Uncertainty	Reference
1	Hg^{2+}	Replicate (manual) denuder measurements	5.7–24 %	Landis et al. (2002)
2	Hg^{2+}	Sample inlet position at ground and on flux tower at 43 m; 92 samples measured	400 %	Lindbergh et al. (1998a)
3	Hg^{0}	Co-located instruments	23 %	Steffen (personal communication, 2011)
4	Hg^{2+}	Co-located measurements	30–40 %	UncertaintyWS2009
5	Hg^{2+} and Hg_p	Co-located measurements, manifold intercomparison study; 3 systems	Hg^{2+}: 10.2 % Hg_p: 31–54 %	Lyman et al. (2009)
6	Hg^{2+} and Hg_p	Incorrect baseline and integration	20 %	Swartzendruber et al. (2009)
7	Hg^{2+}	$HgCl_2$ collection efficiency loss with 50 pbb ozone	12–30 %	Lyman et al. (2010)
8	Hg^{2+}	$HgCl_2$ loss after 30 min ozonation at 30 pbb after collection	40–51 %	Lyman et al. (2010)
9	Hg^{2+} and Hg_p	Estimated total measurement uncertainty	Hg^{2+}: 26 % Hg_p: 33 %	Edgerton et al. (2006)
10	Hg^{0}	Estimated total measurement uncertainty	12 %	Jaffe et al. (2005)
11	Hg^{0}, Hg^{2+} and Hg_p	Emission uncertainty of individual power plants	20–40 %	Edgerton et al. (2006)
12	Hg^{0}, Hg^{2+} and Hg_p	Emission uncertainty by source category	<30 %	Lindberg et al. (1998)
13	Hg^{0}, Hg^{2+} and Hg_p	Air pollution control device used	NA	Wu et al. (2010a)
14	Hg^{2+}	Mercury content of coal burned	100 %	Kim et al. (2010)
15	Hg^{2+}	Modeled emission estimation uncertainty	300 %	Wu et al. (2010b)
16	Hg^{2+}	Reduced levels after in-plume reduction of CFPP compared to UNEP emission inventory	35 %	Deeds (personal communication, 2011)
17	Hg^{2+}	Modeled reduction after adsorption	23 %	Vijayaraghavan et al. (2008)

ACPD
12, 17245–17293, 2012

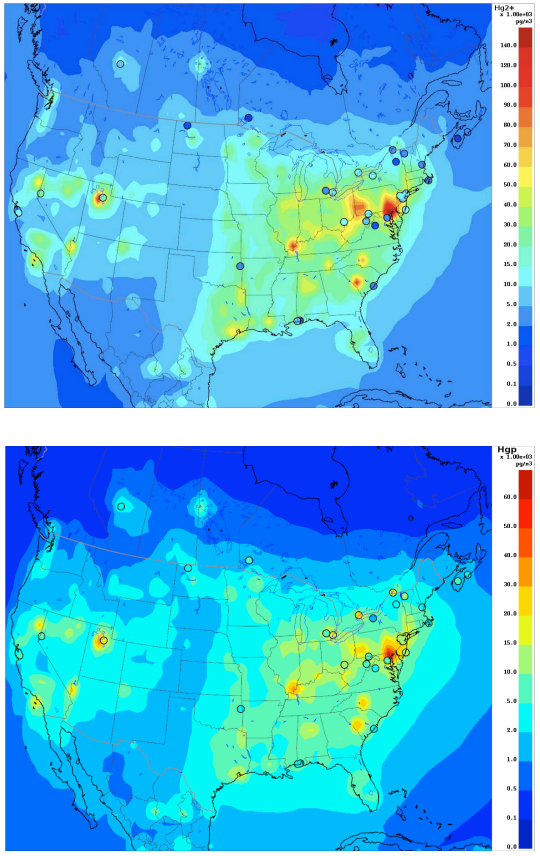

Fig. 1. Comparison of modeled and observed (circles) concentrations for **(a)** Hg^{2+} ($pg\,m^{-3}$); **(b)** Hg_p ($pg\,m^{-3}$) considering emissions only (NoChem; see Table 2 for details). A considerable discrepancy is observed especially in regions of high concentrations.

ACPD
12, 17245–17293, 2012

Measured and modeled oxidized mercury species

G. Kos et al.

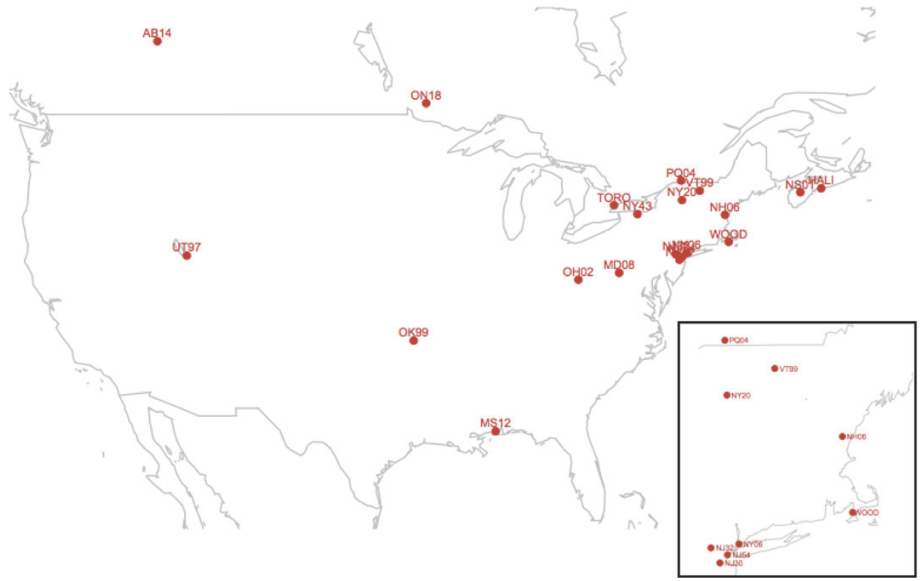

Fig. 2. Location of sites for observations and model estimates sites used in this study. Two site identifiers at the same location indicate co-located instrument data. Zoomed insert shows New Jersey sampling sites resolved. Sampling station at Alert, NU at the northern tip of Ellesmere Island not shown.

ACPD
12, 17245–17293, 2012

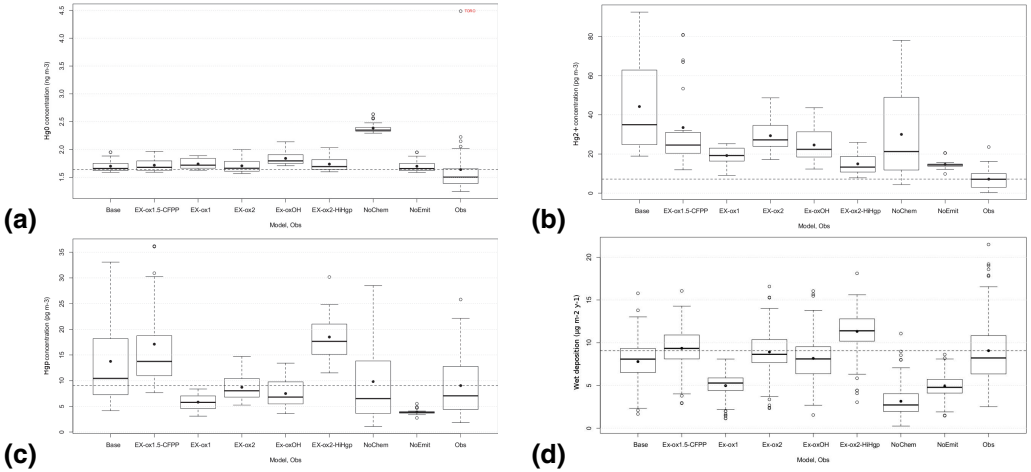

Fig. 3. Spread of yearly means for different model runs and observations. For a detailed model run description see Table 2. **(a)** Hg^0, **(b)** Hg^{2+}, **(c)** Hg_p, **(d)** wet deposition.

ACPD
12, 17245–17293, 2012

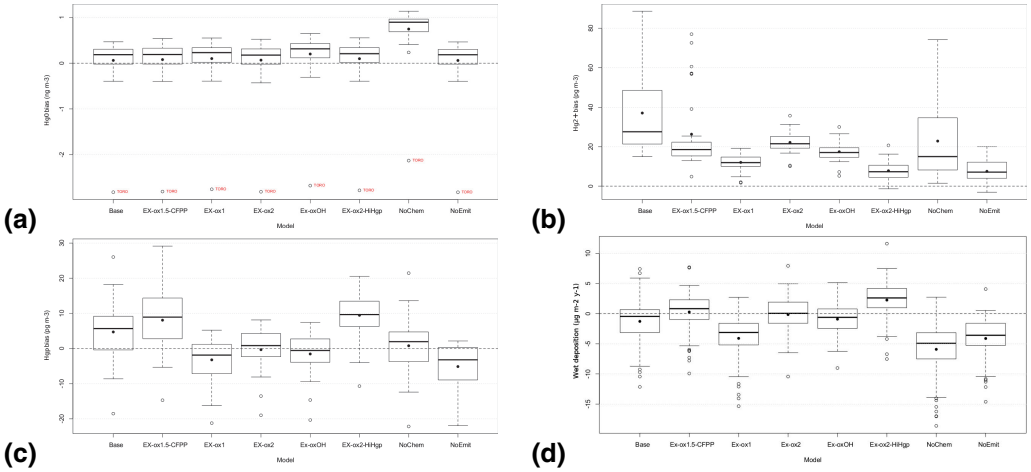

Fig. 4. Spread of yearly bias for different model runs. For a detailed model run description see Table 2. **(a)** Hg^0, **(b)** Hg^{2+}, **(c)** Hg_p, **(d)** wet deposition.

ACPD
12, 17245–17293, 2012

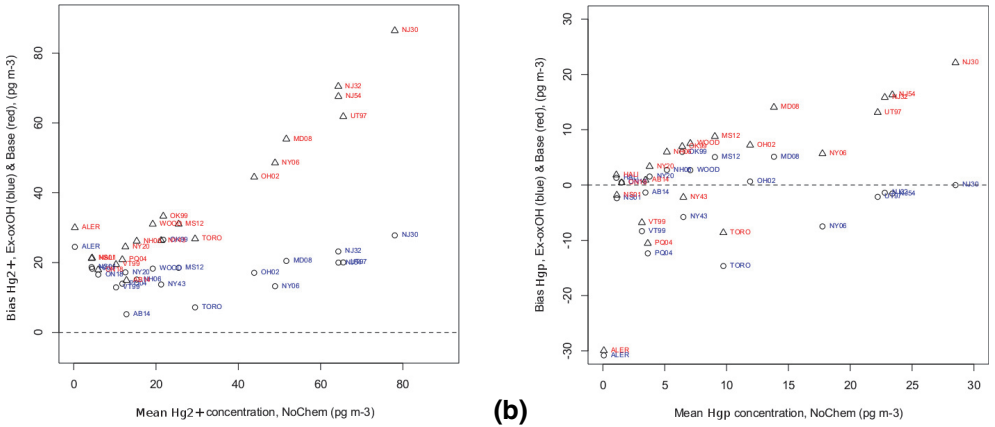

Fig. 5. Model plot of base and Ex-OH bias for **(a)** Hg^{2+} and **(b)** Hg_p at locations with distance from source. On the left are remote stations, on the right stations close to sources.

ACPD
12, 17245–17293, 2012

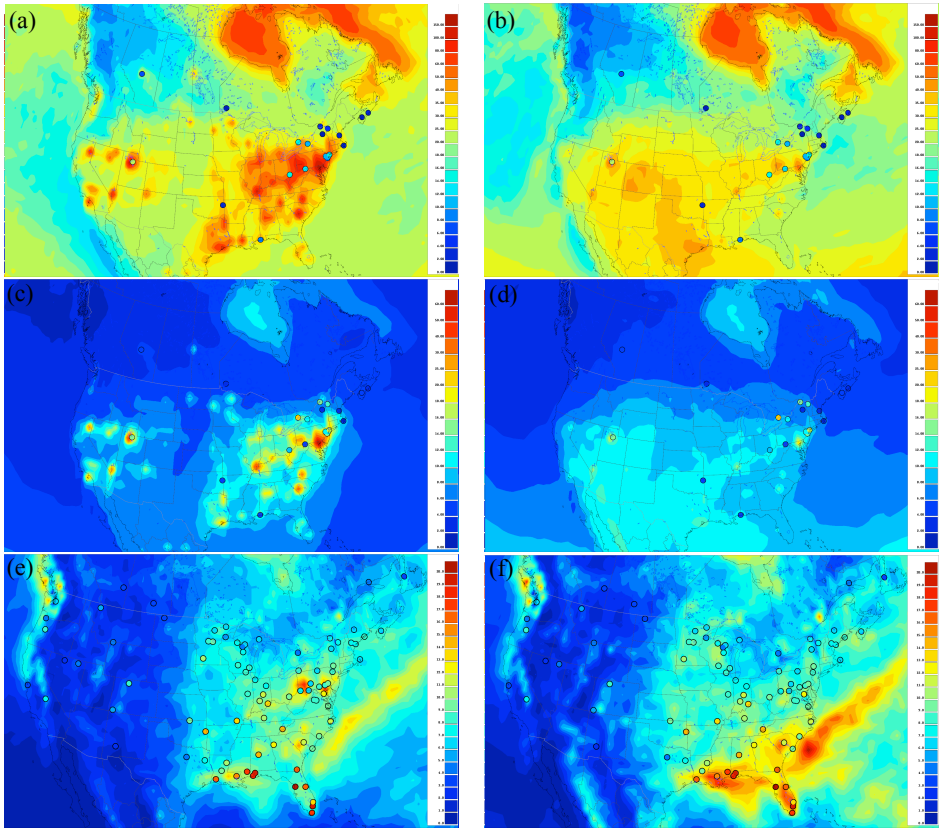

Fig. 6. Model map plots with observations circled. **(a)** base run: Hg^{2+}, **(b)** Ex-oxOH: Hg^{2+}, **(c)** base run: Hg_p, **(d)** Ex-oxOH: Hg_p, **(e)** base run: wet deposition, **(f)** Ex-oxOH: wet deposition. All units for Hg^{2+} and Hg_p in pg m^{-3}. Units for wet deposition are μg m^{-2} yr^{-1}.

ACPD
12, 17245–17293, 2012

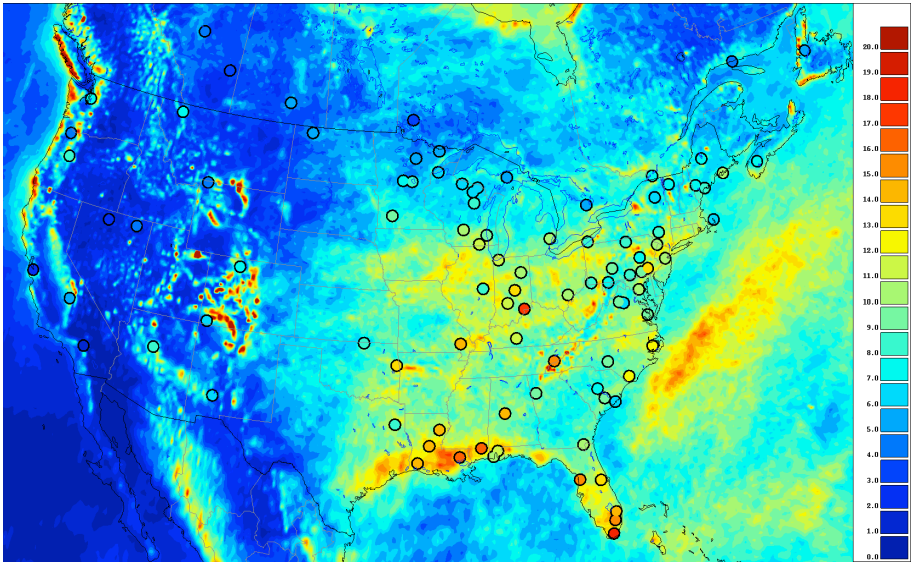

Fig. 7. Ex-oxOH high resolution wet deposition map plots (0.15°; $\mu g\, m^{-2}\, yr^{-1}$) with observations circled for 2006.

ACPD
12, 17245–17293, 2012

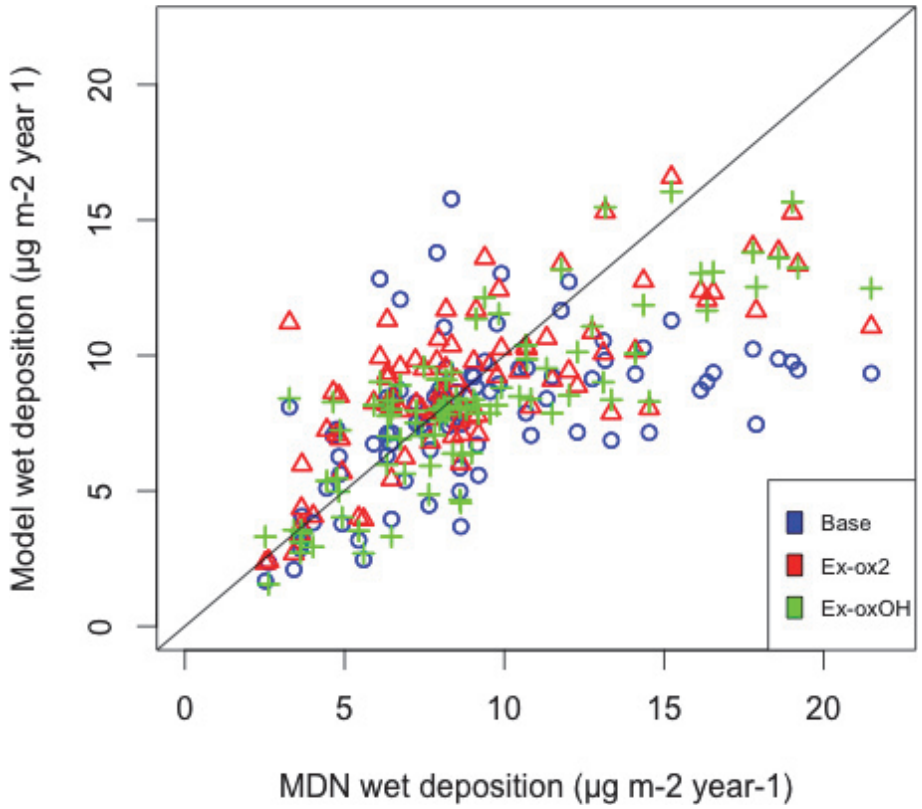

Fig. 8. Yearly averages (2005) of modeled wet deposition concentration plotted against MDN wet deposition measurements.

ACPD
12, 17245–17293, 2012

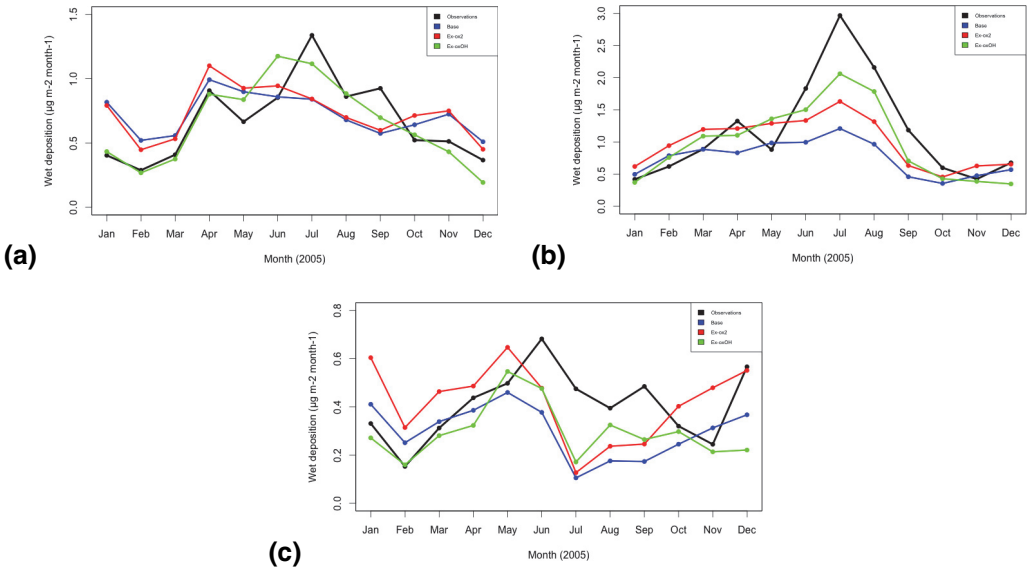

Fig. 9. Comparison of seasonal model estimates with MDN measurement data, all monthly means, for continental regions in North America. **(a)** North East (49 sites) and **(b)** South East (24 sites) are divided by 36° N. **(c)** The western region represents 14 sites from 100° W.

ACPD
12, 17245–17293, 2012